Bernardo Araldi da Silva

Characterization and functionalization of zirconia membranes manufactured by aqueous tape casting

Dissertação submetida ao Programa de Pós-graduação em Engenharia Química da Universidade Federal de Santa Catarina para a obtenção do Grau de Mestre em Engenharia Química
Orientador: Prof. Dr. Dachamir Hotza
Coorientadores: Prof. Dr. Marco Di Luccio
Dr.ª Michaela Wilhelm

Florianópolis
2019

Ficha de identificação da obra elaborada pelo autor através do Programa de Geração Automática da Biblioteca Universitária da UFSC.

Da Silva, Bernardo Araldi

Characterization and functionalization of zirconia membranes manufactured by aqueous tape casting / Bernardo Araldi da Silva ; orientador, Dachamir Hotza ; coorientador, Marco Di Luccio ; coorientadora, Michaela Wilhelm. Florianópolis, SC, 2018.

85 p.

Dissertação (mestrado) - Universidade Federal de Santa Catarina, Centro Tecnológico. Programa de Pós-Graduação em Engenharia Química.

Inclui referências.

1. Engenharia Química. 2. Zircônia. 3. Colagem de fitas. 4. Agentes formadores de poro. 5. Funcionalização. I. Hotza, Dachamir. II. Di Luccio, Marco. III. Wilhelm, Michaela. IV. Universidade Federal de Santa Catarina. Programa de Pós-Graduação em Engenharia Química. V. Título.

Bernardo Araldi da Silva

Characterization and functionalization of zirconia membranes manufactured by aqueous tape casting

Esta Dissertação foi julgada adequada para obtenção do Título de mestre e aprovada em sua forma final pelo Programa de Pós-graduação em Engenharia Química.

Florianópolis, 8 de março de 2019.

_____
Prof[a]. Cintia Soares, Dr[a].
Coordenadora do Programa

_____
Prof. Dachamir Hotza, Dr. Ing.
Orientador
Universidade Federal de Santa Catarina

Banca Examinadora:

_____
Prof. Agenor, De Noni Junior, Dr.
POSENQ/UFSC

_____
Prof. Alan Ambrosi, Dr.
PPGEAL/UFSC

Dedico este trabalho a minha família, que, mesmo longe, sempre ofereceu todo suporte que me era necessário.

AGRADECIMENTOS

Ao meu orientador, Prof. Dr. Dachamir Hotza, por ter depositado a confiança em meu trabalho, por prover todos os elementos necessários para a conclusão deste trabalho e por me mostrar os caminhos quando eles não pareciam tão óbvios para mim.

Ao meu coorientador, Prof. Dr. Marco Di Luccio, por todo o suporte oferecido nas situações adversas durante a realização desse trabalho.

À minha orientadora na Alemanha, Dr. Michaela Wilhelm, pelo conhecimento transmitido e por possibilitar a realização do meu trabalho sob sua supervisão no *Advanced Ceramics Group*.

À Universidade Federal de Santa Catarina (UFSC), em especial ao Programa de Pós-graduação em Engenharia Química (POSENQ), e aos laboratórios:

- LABMASSA, um agradecimento especial à Alexsandra e aos meus colegas de laboratório.
- PROCER, um agradecimento especial ao Marcelo, à Priscila e ao Roberto.
- LCP, um agradecimento especial ao Luiz por todo o suporte oferecido, até mesmo aos fins de semana.

À Central de Análises do EQA.

Ao Prof. Dr. Kurosch Rezwan, por permitir o desenvolvimento do meu trabalho no *Advanced Ceramics Group* e a todo pessoal do IW3.

Aos meus colegas e amigos: Anderson, Yuri, Jean, Jessica, Gabriela, Vinicius e a todos que de alguma forma me impulsionaram até aqui.

Ao Ricardo Cunha, grande amigo que o mestrado me trouxe.

Ao meu avô Pedro, por seu meu exemplo de caráter.

À minha mãe e ao Valmor, por me ensinarem a real definição da palavra “guerreiro”.

A toda minha família, por me auxiliar da forma que fosse possível e por sempre estarem presentes nos momentos mais difíceis.

À CAPES, e em especial ao projeto BRAGECRIM, pelo apoio financeiro.

“Emprega o maior tempo no aperfeiçoamento de ti mesmo, e nenhum tempo em criticar os outros”.

-Carlos Gracie

RESUMO

O objetivo deste estudo foi o desenvolvimento de um sistema de *tape casting* em meio aquoso para produzir membranas porosas de zircônia. Diferentes composições de pastas foram testadas. As propriedades reológicas das suspensões foram medidas. As suspensões mostraram um comportamento pseudoplástico, o que é desejável para um processo de *tape casting*. Dentre as formulações testadas, a pasta com adição de agente formador de poro mostrou-se promissora na produção de membranas com porosidade controlada. As pastas foram coladas por meio de um dispositivo próprio (*doctor blade*), sobre um substrato polimérico (politereftalato de etileno, *Mylar*). Foi investigada, em diferentes temperaturas, a influência do teor de (polimetil-metacrilato, PMMA) sobre porosidade aberta (27% a 51%) e tamanho médio de poros (0.2 a 1.4 μm). Dentre as temperaturas de sinterização, as amostras submetidas a 1400 °C obtiveram o melhor fluxo de permeado, com valores entre 128 e 257 ($L/m^2 \cdot h^{-1}$). A fim de aumentar as propriedades hidrofílicas das membranas, foi realizada uma funcionalização com(3-aminopropril triethoxy silano, APTES). As amostras funcionalizadas foram caracterizadas por SEM-EDX para identificar os grupos funcionais ligados à superfície. Testes do fluxo de permeado foram realizados e valores maiores que 642 ($L/m^2.h^{-1}$) foram encontrados. Pode-se constatar que a porosidade e o tamanho médio de poros têm um papel importante em testes de permeabilidade. Membranas com porosidade e tamanho de poros controlados são indicadas para aplicações em processos de separação, em especial para microfiltração.

Palavras-chave: Zircônia. Colagem de fitas. Agentes formadores de poro. Funcionalização.

RESUMO EXPANDIDO

Introdução

Devido ao alto crescimento populacional, urbanização e industrialização, a contaminação da água aumenta exponencialmente, tornando sua escassez um problema de interesse global (DODDS; PERKIN; GERKEN, 2013; MALWAL; GOPINATH, 2016). Atualmente, a busca por dispositivos de alto desempenho e baixo custo de produção aumentou a demanda por materiais avançados para diversas aplicações. Materiais porosos têm sido amplamente utilizados na vida cotidiana (STUDART et al., 2006b). Um crescente número de aplicações de cerâmicas porosas vem sendo observado nos últimos anos, em ambientes expostos a altas temperaturas e corrosão (KHARISOV; KHARISSOVA; DIAS, 2015). Além disso, devido às suas vantagens sobre membranas poliméricas, as mais utilizadas comercialmente, as membranas inorgânicas vêm se cada vez mais aplicações potenciais no tratamento de água e efluentes. Existem várias rotas sintéticas para fabricar membranas cerâmicas a partir de diferentes matérias-primas. Estes métodos incluem prensagem, eletrofiação, revestimento por imersão, *freeze casting*, *slip casting* e *tape casting* (HASSAN; ABDALLAH, 2016). *Tape casting* (colagem de fitas) é o processo padrão para produção de substratos cerâmicos finos e planos. O processo começa com a preparação de uma suspensão contendo pó cerâmico, solvente e aditivos apropriados, incluindo dispersante, plastificante e ligante (HOTZA; GREIL, 1995). A pasta é moldada sobre uma superfície estacionária ou móvel para formar as filmes, que são então secos até a completa evaporação do solvente. Na sequência, os as fitas ou filmes (*tapes*) são cortados em geometria apropriada, eventualmente laminados, e finalmente submetidas ao processo de *debinding* e sinterização (NISHIHORA et al., 2018b). Técnicas de modelagem em cerâmica, como a extrusão (WERNER et al., 2014), e *tape casting* (MORENO; AGUILAR; HOTZA, 2012) são abordagens simples utilizando sistemas com baixo impacto ambiental e baixa toxicidade que podem produzir cerâmicas com propriedades controladas A zircônia estabilizada com ítria é um dos sistemas mais interessantes para o uso como material de partida. Produtos à base de zircônia são utilizados como cerâmicas estruturais avançadas em coroas dentárias (CHEVALIER, 2006), células a combustível de óxido sólido (SOFC) (MORENO; AGUILAR; HOTZA, 2012) e membranas porosas (BARTELS et al., 2016; HOOG et al. 2018). A microfiltração é um processo físico em que um fluido passa por uma membrana com tamanho de poro controlado. A

faixa de tamanho de poro usada nos processos de microfiltração é de cerca de 0,1 a 10 μm. Sendo assim, o presente estudo foca no desenvolvimento de membranas porosas de zircônia para aplicação em processos de microfiltração.

Objetivos

Os objetivos principais deste trabalho são: produzir, funcionalizar e caracterizar membranas porosas de zirconia produzidas pelo processo de *tape casting* aquoso. Os materiais obtidos são utilizados em processos de microfiltração, cujas propriedades são potencializadas por efeito da A funcionalização.

Metodologia

Para produzir as membranas, pó de zircônia estabilizado com 8 mol% de ítria (8YSZ, zircônia cúbica, - Innovnano com 99,9% de pureza, tamanho médio de partícula de 450 nm e superfície específica de 28,53 $m^{2} \cdot g^{-1}$) foi utilizado. Uma solução comercial de poliacrilato de amônio (Darvan 821 A, Vanderbilt) foi usado como dispersante e uma emulsão de látex estireno-acrílico foi usada como ligante (Mowilith LDM 6138, Clariant), poli(metil metacrilato) (PMMA) com um tamanho médio de partícula de 5 μm foi utilizado como agente formador de poros (PF), dietanolamina como surfactante e uma emulsão aquosa de silicone (Emulsão Y-30, Sigma Aldrich) como agente anti-espumante. Foram preparadas supensões por desaglomeração de pós 8YSZ e PMMA em água desionizada com 1% em peso de dispersante em moinho de bolas. As composições das suspensões foram otimizadas a partir de alguns testes em diferentes quantidades de pó cerâmico (20 a 55% em peso) e estabelecidos com base em conhecimentos prévios do grupo (MORENO; AGUILAR; HOTZA, 2012). Os filmes ou *tapes* foram produzidos em um *tape caster* (CC-1200, Mistler) utilizando um suporte móvel de tereftalato de polietileno (PET, mylar) com um revestimento fino de silicone (G10JRM, Mistler). Os parâmetros de secagem das membranas foram definidos por um planejamento experimental. A temperatura e a umidade relativa que não causaram rachaduras, defeitos ou deformação nos *tapes a* verde foram respectivamente de 20 °C e 85% e, portanto,passaram a ser utilizadas nos demais ensaios. Para sinterização, as temperaturas estudadas foram 1300, 1400 e 1500 °C, respectivamente, com 2 h de patamar nestas temperaturas máximas. A etapa de resfriamento foi fixada em 5 h. Foram realizadas análises de reometria, potencial zeta, porosimetria por intrusão de mercúrio, isotermas de adsorção de nitrogênio, microscopia eletrônica de varredura (MEV) com EDX

(*Energy-Dispersive X-ray spectroscopy*) e adsorção de vapor. A fim de aumentar a hidrofilicidade, foi aplicada a funcionalização da superfície utilizando (3-Aminopropil)trietoxissilano (APTES). Com o objetivo de medir o fluxo de permeado transiente, testes de permeação de água em um dispositivo específico foram realizados antes e após a funcionalização , através de um fluxo vertical ao long da amostra.

Resultados e discussão

As suspensões ou barbotinas mostraram um comportamento pseudoplástico, uma diminuição na viscosidade com o aumento da taxa de cisalhamento, o que é desejável para o processo de *tape casting*. O ponto isoelétrico (IEP) foi encontrado em pH igual a 7,25. Normalmente, a adição de dispersante reduz o IEP e torna a suspensão estável a valores de pH mais baixos. Potenciais zeta maiores que 30 mV em módulo correspondem a suspensões estáveis (HOTZA; GREIL, 1995), as quais promovem a fabricação de fitas cerâmicas homogêneas com resistência a verde e ausência defeitos (REED, 1995). As microscopias revelaram valores de espessura entre 220 e 224 μm para as amostras de zircônia sem agente formador de poros (YSZ_NPF) e em torno de 200 μm para as membranas com PF (YSZ_PF). Um tamanho médio de poros variando entre 0,3 μm e 1,4 μm foi obtido. A adição do PF (PMMA) ajudou a evitar a alta densificação. A porosimetria de intrusão de Hg mediu a distribuição média do tamanho dos poros e a porosidade apresentada nas membranas. A porosidade aberta variou em um intervalo entre 27% e 51%, de acordo com o uso de PMMA e a temperatura de sinterização. Excluindo as baixas frações de poros grandes, todas as amostras mostraram uma distribuição simétrica de poros entre 0,1-1,5 μm. Em membranas simétricas, a espessura de toda a membrana determina o fluxo que passa por ela. Isotermas de adsorção de nitrogênio e área superficial específica (ASE) das membranas sinterizadas foram investigadas para determinar a influência do tempo de sinterização na microestrutura. A ASE obtida para as amostras sinterizadas em três temperaturas diferentes apresentaram valores de 0,24 a 1,74 m^2/g. Todas as isotermas podem ser classificadas como tipo II, o que é típico para sólidos macroporosos (<50 nm) mostrando preenchimento de macroporos, mas sem adsorção multicamadas. Espectros de EDX mediram a composição antes e depois da funcionalização, evidenciando o sucesso na deposição de APTES na superfície da membrana. A adsorção de vapor de solvente polar (água) e não polar (n-heptano) foi realizada para determinar as propriedades da superfície da membrana. Todas as amostras apresentaram um

comportamento hidrofílico que é comum para cerâmicas óxidas. A medição de permeação de água foi realizada em um dispositivo sem saída em três diferentes pressões de trabalho (0,5, 0,75 e 1 bar). Os testes revelaram que embora a porosidade desempenhe um papel na permeabilidade dasmembranas, o tamanho médio dos poros parece ter uma influência mais forte no fluxo de permeado. Após o procedimento de funcionalização, o desempenho das membranas foi avaliado. As membranas apresentaram fluxos 5 vezes maiores quando comparadas com as mesmas amostras antes da funcionalização. Quando a superfície é modificada com APTES, grupos amino (NH_2) são fixados na superfície da membrana, os quais tendem a aumentar a interação com a água e facilitar a permeação da água pelos poros.

Conclusões

Neste trabalho, membranas porosas de zircônia estabilizada com ítria foram produzidas com sucesso pelo processo de *tape casting*. O pH no ponto isoelétrico foi de 7,25 para a suspensão de zircônia. A pasta cerâmica a pH 9 corresponde a um potencial zeta de -45 mV, confirmando que a barbotina é coloidalmente estável. O comportamento reológico da suspensão foi pseudoplástico, o que é desejável para um processo de *tape casting*. O valor da área superficial específica corresponde a resultados publicados na literatura. Membranas com porosidade aberta de 27% a 51% e tamanhos de poros na faixa de 0,2 a 1,5 μm foram obtidas. A adsorção de água e vapor de n-heptano mostrou que as membranas apresentam um comportamento hidrofílico. A etapa de funcionalização foi realizada com sucesso e confirmada por análise elementar de MEV-EDX. As membranas funcionalizadas mostraram um aumento do fluxo de água em até 5 vezes. O tamanho médio dos poros e a porosidade desempenharam um papel significativo na permeação de água, tanto para amostras funcionalizadas como não funcionalizadas. No entanto, o tamanho médio dos poros parece ter uma influência mais forte do que a porosidade. A faixa de porosidade indicou uma potencial aplicação dessas membranas para processos de microfiltração.

Palavras-chave: Zircônia. Membrana. Funcionalização. Microfiltração.

ABSTRACT

The objective of this study was the development of tape casting in aqueous medium to produce porous zirconia membranes. Different slurries compositions were tested. The rheological properties of the suspensions were measured. The suspensions showed a pseudoplastic behavior, which is desirable for tape casting. Among the formulations tested, the slurry with addition of pore forming agent showed to be promising in the production of membranes with controlled porosity. The slurries were cast with a tape caster (doctor blade) on a polyethylene terephthalate (Mylar) substrate. The influence of (poly(methyl-methacrylate) PMMA) content, at different temperatures (1300°C, 1400°C, 1500°C) on open porosity (27% to 51%) and mean pore size (0.2 to 1.4 μm) was investigated. Among the sintering temperatures, the samples submitted to 1400 ° C obtained a better permeate flux, with values between 128 and 257 ($L/m^{2}{\cdot}h^{-1}$). In order to increase the hydrophilic properties of the membranes, (3-aminopropril triethoxysilane, APTES) functionalization was performed. The functionalized samples were characterized by SEM-EDX to qualify the functional groups attached to the surface. Permeate flow tests were performed and values higher than 642 ($L/m^{2}{\cdot}h^{-1}$) were found. It can be concluded that porosity and mean pore size play an important role in permeability tests. Membranes with controlled porosity and pore size are indicated for applications involving separation processes, in special for microfiltration systems.

Keywords: Zirconia. Tape casting. Sacrificial pore former. Functionalization.

LIST OF FIGURES

LIST OF TABLES

LIST OF ABBREVIATIONS

APTES	Aminopropyltriethoxysilane
BET	Brunauer, Emmet and Teller
DLS	Dynamic light scattering
IEP	Isoelectric point
MLC	Multi-layer capacitors
MLCP	Multi-layer ceramic packing industry
MSS	Monoclinic solid solution
NaCMC	Sodium carboxymethyl cellulose
PET	Poly (ethylene terephthalate)
PMMA	Poly (methyl methacrylate)
PSZ	Partially stabilized zirconia
PVB	Polyvinyl butyral
RT	Room temperature
SEM	Scanning electron microscopy
TSS	Tetragonal solid solution
TSZ	Totally stabilized zirconia
YSZ	Yttria stabilized zirconia
8YSZ	8 mol yttria-stabilized zirconia

LIST OF SYMBOLS AND UNITS

A	Cross-sectional area of the sample	[mm^2]
A_m	Effective membrane surface area	[mm^2]
dt	Differential time	[s]
dV	Differential volume	[mL]
J	Transient permeate flux	[$L \cdot m^{-2} \cdot h^{-1}$]
k	Specific permeability	[m^2]
L	Length of the sample	[mm]
M_w	Molar weight	[$kg \cdot mol^{-1}$]
p	Absolute pressure	[bar]
p_m	Measured pressure	[bar]
p_0	Initial pressure	[bar]
r	Radius	[mm]
U_A	Potential attraction energy	[$J \cdot kg^{-1}$]
V	Volume of total adsorbed gas	[L]
V_m	Volume of adsorbed gas	[L]
α	Contact angle	[°]
γ	Surface tension	[$N \cdot m^{-1}$]
μ	Viscosity of the fluid	[$Pa.s^{-1}$]
ΔP	Hydrostatic pressure drop	[bar]

SUMMARY

1 INTRODUCTION

1.1 MOTIVATION

Due to high population growth, urbanization and industrialization, water contamination increases exponentially, making its scarcity a problem of global interest (DODDS; PERKIN; GERKEN, 2013; MALWAL; GOPINATH, 2016). The water scarcity is one of the most serious risks facing the world at every level. Different efforts to provide treated water to a growing population have been done, which emphasize the need to manage and treat the natural resource in a sustainable way.

Currently, the pursuit of high-performance devices with low cost of production has increased the demand for advanced materials for several applications. Macroporous materials have been widely used in everyday life, including polymeric foams, aluminum light-weight structures in buildings and airplanes as well as porous ceramics for water purification (STUDART et al., 2006b).

An increasing number of applications of porous ceramics can be observed to date, regarding applications in environments where high temperatures and corrosive media are involved. Molten metals filtration, hot corrosive gases, support for catalytic reactions and high temperature thermal insulation are included in such use (KHARISOV; KHARISSOVA; DIAS, 2015). Moreover, due to their advantages over commercially widespread polymeric membranes, inorganic membranes have been increasingly gaining potential applications in the water and wastewaters treatment.

The main advantages of ceramic membranes are their high melting point, conferring them high thermal resistance; high chemical stability, which favors their application in corrosive media and in organic solvents; as well as high specific strength and wear resistance. In addition, they show low thermal conductivity, low dielectric constant and good water permeability (ASHARAF et al., 2014). There are various synthetic routes for fabricating ceramic membranes from different raw materials. These methods include pressing, extrusion, sol- gel, chemical vapor deposition, electro spinning, anodic oxidation, dip coating, freeze casting, slip casting and tape casting (HASSAN; ABDALLAH, 2016).

Tape casting is the standard process to thin and flat ceramic substrates. The process begins with the preparation of a suspension containing the ceramic powder and solvent, with the appropriate additives, including dispersant, plasticizer and binder (HOTZA; GREIL,

1995). The dispersant keeps the ceramic particles apart, avoiding agglomeration while the plasticizer and the binder promote flexibility and resistance to the green ceramic body, respectively. The slurry is cast on a stationary or mobile surface to form the tapes, which are then dried until complete solvent evaporation. In the sequence, the pieces are cut into appropriate geometry, eventually laminated, and finally submitted to debinding and sintering (NISHIHORA et al., 2018b).The tape casting process was originally employed industrially based on organic solvents. Although, due to health, disposal, safety, cost and environmental issues, researchers are focusing on aqueous systems that have the water use benefits (GOULART; SOUZA, 2017). The main advantages of water are its non-toxicity, anti-flammability, high availability and low cost (BELON et al., 2019; MARIE et al., 2017). On the other hand, organic additives affect the suspension behavior and the properties of the tapes. Thus, the composition of the slips should be optimized to obtain crack-free tapes with high green density and controlled porosity.

Ceramic shaping techniques, such as water-based extrusion (WERNER et al., 2014), and tape casting (MORENO; AGUILAR; HOTZA, 2012) are simple approaches using systems with low environmental impact and low toxicity that can produce ceramics with controlled properties. In the case of porous ceramics, pore sizes ranging from nano to micrometers might be obtained, with the use of different porogenic agents, resulting in ceramic materials with superior performance to other manufacturing techniques.

Among the oxides, yttrium-stabilized zirconia is one of the most interesting systems for using as ceramic starting material. Zirconia-based products are used as advanced structural ceramics in tooth crowns (CHEVALIER, 2006), solid oxide fuel cells (SOFC's) (MORENO; AGUILAR; HOTZA, 2012) and porous membranes (ALBANO et al., 2008) due to their high toughness (BARTELS et al., 2016; HOOG et al., 2018).

Microfiltration is a physical process where a fluid pass through a special pore-sized membrane. It usually serves as a pre-treatment for other separation processes such as ultrafiltration. The particle size range used in microfiltration processes are from about 0.1 to 10 μm.

Therefore, the present study focused on the development of zirconia membranes for application in microfiltration processes.

1.2 OBJECTIVES

1.2.1 General objective

The general objective of this work is to produce and characterize zirconia microfiltration membranes obtained by aqueous tape casting and combine this well-established technique with functionalization a step to enhance the membrane water permeability.

1.2.2 Specific objectives

a) Produce zirconia membranes by aqueous tape casting with controlled porosity and thickness ranging inside the microfiltration range;

b) Functionalize the porous membranes to increase hydrophilicity;

c) Characterize the membrane morphology, hydrophilicity and water permeability;

2 THEORETICAL BACKGROUND AND LITERATURE REVIEW

2.1 CERAMICS

Ceramic materials are composed of metallic and nonmetallic elements, often as oxides, carbides and nitrites. The wide variety of materials under this classification includes ceramics that are fabricated from clay minerals, cement, and glass. These materials are typically insulating to the passage of electricity and heat. They are more resistant to high temperatures and abrasive environments when compared to metals and polymers (CALLISTER JR., 2002).

2.1.1 ZIRCONIA CERAMICS

Zirconia (ZrO_2, zirconium dioxide) is the most important and stable oxide derived from zirconium. This metal oxide can be extracted from zirconite ($ZrSiO_4$) or from baddeleyite (ZrO_2) (OLIVEIRA; TOREM, 2001). In its pure form is a white powder and has a melting point of 2710 °C, and may be found in three crystalline forms (FLETCHER ANDREW, 1993): monoclinic, tetragonal or cubic.

Zirconia-based ceramics are characterized by a combination of some properties such as chemical resistance, mechanical strength, and toughness. This allows the use of this material in aggressive environments, and as cutting tools. Zirconia is also considered an attractive material for nuclear, chemical, aerospace, fuel cell and biomaterials applications (ASHARAF et al., 2014; REED, 1995).

2.1.1.1 Binary phase balance

Zirconia presents a few phase transformations. The total change from tetragonal to cubic occurs at 2370 °C. Another common change is from tetragonal to monoclinic phase, and when it happens, it results in large shear deformations because of the density shift. These deformations, even in small grains are sufficient to exceed both elastic and fracture limits. In this case, the use of pure zirconia oxide components at high temperatures is difficult as it is related to increased stress and spontaneous

failure. The volume change accompanying the tetragonal to monoclinic phase transformation may, however, be an alternative to improve the strength and toughness of zirconia (ALBANO et al., 2009).

These oxides may exhibit degradation in dry and humid atmospheres over a temperature ranging from 65 to 500 °C. This degradation is due to the destabilization of the tetragonal phase to monoclinic. Therefore, its application is intended for situations where mechanical resistance is the property of interest.

A common oxide for the stabilization of zirconia is the yttrium oxide (Y_2O_3), which confers better fracture toughness (SENTHIL KUMAR; RAJA DURAI; SORNAKUMAR, 2004).

The scientific and technological interest in stabilized zirconia ceramics is large mainly due to their mechanical behavior. Zirconia stabilization can be partial or total and it is controlled by the amount of phase stabilizing oxides that are added to the matrix. Stabilized zirconia is generally found as: i) Partially Stabilized Zirconia (PSZ), which contains stabilizing additives sufficient to allow the formation of tetragonal zirconia precipitates in a cubic matrix, consisting of amounts greater than 4 mol% Y_2O_3 , or ii) Fully Stabilized Zirconia (FSZ) with about 100% of the tetragonal crystalline phase at room temperature, containing 8 mol% Y_2O_3, commonly(ASHARAF et al., 2014). High toughness in zirconia is related to the martensitic transformation and the increase of the molar fraction of Y_2O_3 in the material favoring the stabilization of the cubic phase, as shown in Fig. 1.

Fig. 1 - Zirconia-Yttrium phase diagram for yttrium additions up to ~ 20 mol% Y_2O_3. (T) tetragonal phase, (C) cubic and (M) monoclinic.

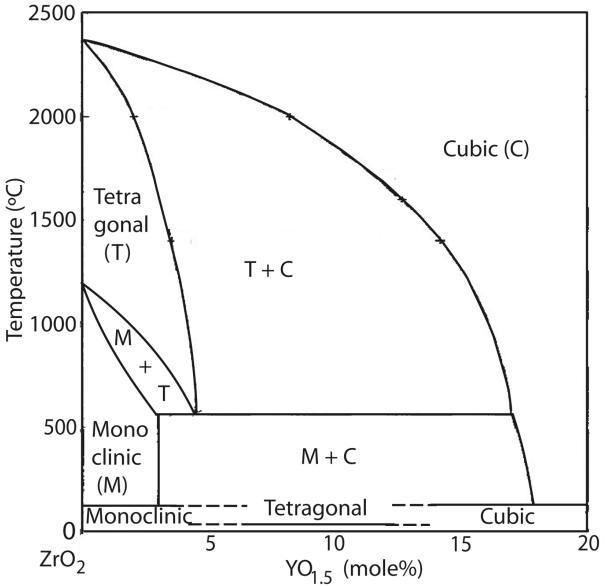

Source: (WITZ et al., 2007).

2.1.1.2 Martensitic transformation

The transformation of the zirconia particles from the tetragonal to monoclinic phase is of the martensitic type and is accompanied by a 3 to 5% volume increase. This volume is sufficient to exceed the elastic limit even in small grains of monoclinic zirconia, and this expansion of volume can only be accommodated by the formation of cracks, making it impossible to use the zirconia in its pure form. The additions of some oxides make it possible to obtain suitable mechanical properties (FLETCHER ANDREW, 1993). The transformation is thermodynamically reversible at a temperature of 1174 °C. This transformation begins in the cooling cycle at the martensitic transformation temperature, which for ZrO_2 monocrystals or dense bodies of polycrystalline ZrO_2 is between 950 °C and 850 °C.

The most important characteristic in the ZrO_2-Y_2O_3 system is the decreasing of the tetragonal-monoclinic transformation temperature with the increasing in the amount of yttrium. Thus, larger particles of ZrO_2 stabilized with Y_2O_3 may be retained in their tetragonal form which is

metastable (FLETCHER ANDREW, 1993). Therefore, by adding yttria to zirconia, the martensitic transformation is inhibited (HEUER, 1987).

2.1.2 NANOSTRUCTURED ZIRCONIA CERAMICS

The use of nanometric scale ceramic powders is becoming an attractive option due to the unique properties associated with its nanostructure. The advantage of these powders is their reactivity, the challenge is to obtain dense or porous ceramics, depending on the application (MINEIRO, 2008).

Among the ceramic materials used for high performance, zirconia-based ceramics have the greatest potential for application. This potential is linked to the combination of its mechanical, optical, chemical, electrical and thermal properties, and thus make oxides an attractive choice in materials science because of their well-known phase transformations and the microstructure development (ASHARAF et al., 2014).

A study published by Studart et al., (2006b) demonstrated that zirconia nanoparticles have great potential as a starting material for applications in technological field. Among them refers to fabrication of ceramic membranes targeting microfiltration processes (BOUZERARA et al., 2012).

2.1.3 ZIRCONIA CERAMICS FOR STRUCTURAL APPLICATIONS

High-performance ceramics are potential substitutes for conventional materials. In order to obtain micro structured ceramics with properties compatible with their use, it is necessary for this microstructure to have suitable chemical and physical characteristics. The goal, therefore, is to obtain a sintered ceramic with the smallest defect size possible, so that the reliability and reproducibility of the properties in the performance of the final ceramic product are guaranteed.

Ceramic materials are characterized by strong atomic bonds of ionic and covalent character between their atoms. The nature of these bonds is responsible for some highly desirable properties of these materials, such as hardness and high melting point, abrasion resistance and chemical stability. However, these high energy bonds make these

materials to exhibit a brittle mechanical behavior (ASHARAF et al., 2014).

In order to enhance the reproducibility and reliability of these materials, microstructures have been developed to increase fracture toughness and rupture strength, in order to tolerate a certain amount of natural defects (FLETCHER ANDREW, 1993). In structural applications, the main limitation of ceramics is not mechanical resistance or limited rigidity, but rather the fragility with which cracks start and propagate (CHEVALIER et al., 2009).

It is known that cracks start in defects that are introduced during the manufacturing process, and may be generated by inclusions, dense clumps or pores as well as during surface finishing such as grinding and polishing and also exposure to mechanical aggressive environments. However, cracks can be disrupted when their energy is consumed, such as when they meet grain boundaries or barriers, or when a phase transformation occurs at the crack tip (SENTHIL KUMAR; RAJA DURAI; SORNAKUMAR, 2004).

Zirconia undergoes an increase in its mechanical resistance when subjected to the action of an external force applied at room temperature that increases its resistance to mechanical shocks (FLETCHER ANDREW, 1993). This special property is allied to the transformation of the tetragonal to the monoclinic phase, which is accompanied by an increase in volume, causing a state of internal compression in the material. When a crack begins to propagate inside the ceramic, the energy associated with this state of compression in the region near the tip of the crack is absorbed by the ceramic object, minimizing or interrupting the propagation of the defect (CHEVALIER et al., 2009).

The retention of the metastable tetragonal phase and its consequent transformation to the monoclinic phase is considered a prerequisite for the increase of the fracture toughness of zirconia ceramics, making it a material with great potential for the application as microfiltration ceramic membranes (BOTHA, P. J.; CHIANG, J. C. H.; COMINS, J. D.; MJWARA, P. M.; NGOEPE, 1998; FLETCHER ANDREW, 1993).

2.1.4 ZIRCONIA MEMBRANES MATERIALS AND DESIGNS

Zirconia membranes have been employed in different applications such as solid oxide fuel cells (BAQUERO et al., 2013), virus retention (WERNER et al., 2014) and water microfiltration (BOUZERARA et al.,

2012). Table 1 summarizes some of the most common techniques used in zirconia membrane manufacturing and their applications.

Table 1 - List of most common zirconia membranes manufactured and their applications.

Material	Technique	Membrane Design	Pore geometry	Porosity (%)	Average pore size (μm)	Application	Reference
Zirconia (ZrO_2)	Extrusion	Tubular	-	60	0.1	Oil/water emulsion	(BEROT et al., 2003)
3YSZ	Extrusion	Tubular	Irregular spheroidal shape	29.5 - 55.2	0.2	Bacteria filtration	(KROLL et al., 2010)
ZrO_2 membranes supported in clay and calcium carbonate	Extrusion	Tubular	Irregular spheroidal shape	-	0.16	Water microfiltration	(BOUZERARA et al., 2012)
3YSZ	Extrusion	Tubular	Irregular spheroidal shape	50	-	Bacteria filtration	(KROLL et al., 2012)
3YSZ	Extrusion	Tubular	Irregular spheroidal shape	46.6 – 51.8	0.5 – 0.2	Virus retention	(BARTELS et al., 2016)
3YSZ	Extrusion	Tubular	Irregular spheroidal shape	49.79 – 53.79	0.084 – 0.108	Enzyme functionalization	(TAJIRI, 2018)
ZrO_2 supported in kaolin	Colloid filtration technique/sol-gel	Tubular	Irregular shape	-	0.1	Heavy metals separation	(CHOUGUI et al., 2014)
3YSZ	Electrospinning	Tubular	Irregular shape	-	1.8 – 2.7	Water microfiltration	(YI; WANG; LI, 2017)
8YSZ	Aqueous tape casting	Flat	Irregular spheroidal shape	-	0.09	Water micro and ultrafiltration	(ALBANO; GARRIDO, 2006)

Source: Elaborated by the author (2019).

Table 1 - List of the most common zirconia membranes manufactured and their applications (continued).

8YSZ	Aqueous tape casting	Flat	Irregular spheroidal shape	33	11	-	(ALBANO et al., 2008)
8YSZ	Aqueous tape casting	Flat	Irregular spheroidal shape	6.9	-	Solid oxide fuel cell (SOFC)	(MORENO; AGUILAR; HOTZA, 2012)
8YSZ-NiO	Tape casting	Flat	Irregular spheroidal shape	83.4	1	Solid oxide fuel cell (SOFC)	(BOARO et al., 2003)
8YSZ	Tape casting	Flat	Irregular spheroidal shape	-	0.3	Solid oxide fuel cell (SOFC)	(BAQUERO et al., 2013)
8YSZ-NiO	Tape casting	Flat	Irregular spheroidal shape	26.8 –48.3	0.27 – 0.45	Supporting anode for SOFC	(SANSON; PINASCO; RONCARI, 2008)
8YSZ	Tape casting	Flat	Irregular spheroidal shape	35	2 – 200	-	(SARIKAYA; DOGAN, 2013)
ZrO_2 supported on Titania (TiO_2)	Tape casting	Flat	-	-	0.45 – 1.4	Oil/water emulsion	(MATOS et al., 2013)

3YSZ: yttria-stabilized zirconia (3 mol%), 8YSZ: yttria-stabilized zirconia (8 mol%).

Source: Elaborated by the author (2019).

Table 1 shows that the use of zirconia as starting material has a broad application in different areas such as microfiltration and ultrafiltration membranes (ASHARAF et al., 2014). The use of zirconia membranes was successfully applied in solid oxide fuel cells (MORENO; AGUILAR; HOTZA, 2012; BAQUERO et al., 2013) using zirconia membranes manufactured by tape casting. Some studies applied extruded membranes for virus removal (BARTELS et al., 2016) with a membranes flux of 150 L/(m^2·h) and bacteria filtration (KROLL et al., 2012) showing a bacterial retention of 99.9%.

Zirconia membranes are also reported in wastewater treatment. Membranes manufactured by sol-gel technique and extrusion are applied in separation of heavy metals (CHOUGUI et al., 2014) and oil/water emulsions (BEROT et al., 2003) even though a large number of studies on water and wastewater treatment were recently published, a lack of research related to developing techniques such as tape casting can be noticed.

Therefore, this work aims to explore the correlation between the well-established tape casting technique combined with surface functionalization to fill in the gap presented in this area.

2.2 TAPE CASTING

The tape casting process has been the standard technique for manufacturing of ceramic tapes in large scale, with tape thickness ranging from 2 micrometers up to the order of millimeters (MISTLER; TWINAME, 2000). This method allows processing different types of raw materials regardless their composition from ceramic, vitreous or metallic powders. It is considered a fundamental technique by the industries of fuel cell production, multilayer packages and water and wastewater technology (JABBARI et al., 2016).

The first study about tape casting was published by Glenn Howatt (1947), as a method of forming thin plates for piezoelectric application and capacitors. The first patent, though, was published in 1952. This discloses the use of aqueous and non-aqueous suspensions using a movable device provided with a blade in a discontinuous process (PLATES, 1952). In 1961, the company American Lava Corp. filed a patent describing the use of a mobile polymer matrix of a ceramic suspension containing polyvinyl butyral (PVB), which was cast with the

help of a system consisting of leveling blades, so-called doctor blades (MISTLER; TWINAME, 2000).

At the beginning of the twentieth century, the tape casting technology went through an optimization. Several researches have been carried out in the area of dispersants for the suspension, with the intention to use nanopowders (GESELLSCHAFT.; EMAILFACHLEUTE., 1920; STUDART; AMSTAD; GAUCKLER, 2007; MORENO; BERNARDINO; HOTZA, 2014).

The process consists in the preparation of a suspension with the raw material of interest in the aqueous or non-aqueous medium. Additives such as binders, plasticizers, antifoams, and surfactants are part of the suspension, each promoting its specific function (HOTZA, 1997).

The non-aqueous process where the medium is an organic solvent offers some advantages such as high and fast solvent volatility and these solvents avoid hydration and hydrolysis of the ceramic powder. However, these solvents are usually constituted by toxic substances, thus requiring a rigid control of the products of their decomposition that are emitted into the atmosphere. Considering this, a great number of studies have been developed aiming at the consolidation of some alternatives based on aqueous systems (ALBANO; GARRIDO, 2006; ALBANO et al., 2008; ALBANO et al., 2009; COSSIO et al., 2012; DONG et al., 2017).

Tape casting is a process similar to slip casting. In addition, many of the processing problems are common in both. However, in slip casting the solvent removal during product consolidation involves the capillary action of a porous mold, while in tape casting the solvent is simply evaporated. The size and shape of the products manufactured by both differ considerably (HOTZA; GREIL, 1995; JABBARI et al., 2016; NISHIHORA et al., 2018b).

Tape casting, Fig. 2, is performed through the relative movement between a doctor blade and a collecting surface. There are two possible approaches: either a blade moves on a surface (discontinuous process) or a surface moves under a fixed blade (continuous process). Large-scale production is based on continuous processes. For production on pilot scales or laboratory scales, the batch process can be used (MISTLER; TWINAME, 2000). Industrially, the standard equipment consists of a movable surface, hot air flow drying system, leveling blade device and a separating system between the green leaf and the substrate (HOTZA, 1997). The substrates are often made from Teflon, cellulose acetate and polyethylene (MISTLER; TWINAME, 2000).

Fig. 2 - Tape caster for continuous processing of ceramic tapes.

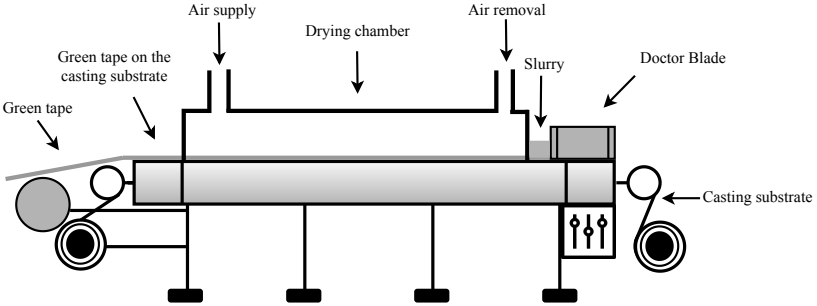

Source: Elaborated by the author (2019).

The tape thickness control can be adjusted by the doctor blade relative to the collector surface, varying in the micrometer range. Other parameters such as the viscosity of the suspension, pressure exerted by the suspension in the reservoir and the casting speed also influence the thickness of the film. The bonding speed in continuous equipment varies from 5 to 1000 mm/min. Such speed depends on the drying conditions and the required production (NISHIHORA et al., 2018b).

After evaporation of the solvent, the ceramic particles dispersed in the polymer matrix give rise to a flexible tape. This can be separated from the substrate manually. The tape must have adequate flexibility, density, and mechanical strength to allow better handling and storage without inducing defects (MISTLER; TWINAME, 2000).

After processing, the material is subjected to a heat treatment, which can be performed in one or two steps. The first step is debinding, which aims at the elimination of organic substances. The second is the sintering which promotes the densification of the material.

The steps for preparing the ceramic tapes are described in Fig. 3.

Fig. 3 - Flowchart of the ceramic tapes manufacturing process.

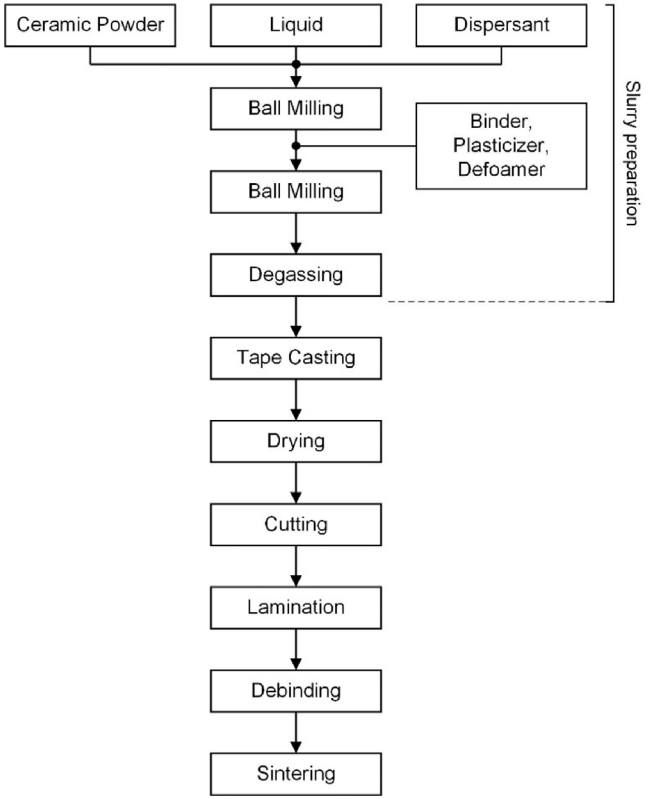

Source: Nishihora et al. (2018).

In the following topics, the intrinsic aspects of the processing of the ceramic tapes in the aqueous medium will be briefly discussed. Although the processing of ceramic powders in aqueous media is one of the oldest and studied routes within ceramic processes, there are still some difficulties to be overcome regarding the achievement of stabilized aqueous suspensions with high solids and homogeneously dispersed as well as a controlled drying of the tape so as to avoid cracks (JABBARI et al., 2016).

2.2.1 SLURRY RHEOLOGY

Rheology is defined as the study of the fluid behavior and the deformation of this material when it is subjected to a certain external mechanical stress (CHHABRA, 2010). There are different parameters that can influence the stability of a suspension of ceramic powders. Among them, the ionic strength, nature of the additives, temperature, solid loading and the presence or absence of oxides (TARÌ; OLHERO; FERREIRA, 2000).

There is a great variation in the formulations used in ceramic tapes. This suggests that the materials obtained in industrial processes present a varied behavior. To process these materials, the knowledge of the properties and operating conditions is required. Some simple variations such as rate of application of pressure and amount of organic additive employed may alter the rheological behavior of a ceramic suspension (CHHABRA, 2010).

In the processing of ceramic materials, some flow characteristics are desirable. For example, the pseudoplastic character of the organic additive may favor the pseudoplastic behavior of the whole suspension. In other words, the viscosity of the ceramic slurry is reduced as the applied shear rate increases, facilitating the deformation process (MISTLER; TWINAME, 2000).

Flow properties are as important for advanced ceramics as for traditional ones because it is not possible to predict this behavior by analyzing the characteristics of the precursors involved as a function of the complexity of the relationships between the components or a suspension. However, an analysis of similar material can be used, allowing a prediction of the behavior of the suspension (HOTZA; GREIL, 1995) . It may be suggested that a modification in the flow profile promotes changes in the viscosity of the suspension.

The main factors that influence the viscosity of the suspension are temperature, solid loading and solvent characteristics (ÖZKAN et al., 1999). Each suspension has a limit concentration of solids. At this limit, the agglomeration takes place and the flow is ceased. When the increase in solids concentration occurs, deviations from Newtonian rheological behavior occur. In this case, the behavior of the suspension depends on additional factors, such as type of interaction between particles (repulsion or attraction), particle size, density, form and specific surface area.

Fig. 4 shows the influence of particle size on the suspension flow. In Fig. 4 (a) there are no particles dispersed in the fluid, making the flow continuous. In Fig. 4 (b) a particle exhibits a certain resistance to the passage

and flow of the fluid. In (c) this resistance is greater since the particle size also increases. Fig.4 (d) shows how a set of small particles behaves as a single large particle when agglomerated, which generates resistance to fluid flow (CHHABRA, 2010).

Fig. 4 - Influence of the presence of bound particles on the flow lines.

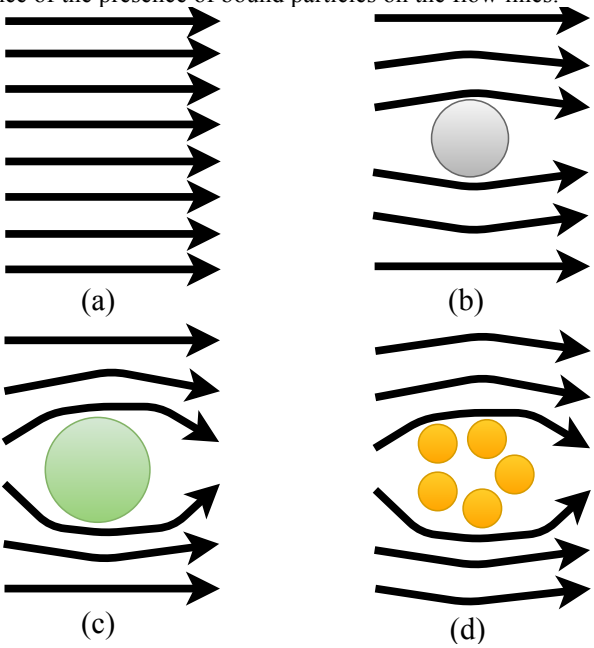

Source: Adapted from (RODRIGO; PARDO, 2005).

Some possible behaviors for fluids are discussed in Fig. 5. The rheological behavior of the fluids does not always present a linear relationship between shear stress and shear rate as Newtonian fluid. Thus, the apparent viscosity, defined by the ratio between stress and shear rate, depends not only on the shear rate but also on other factors, such as time (STUDART et al., 2006a).

Fig. 5 - Basic rheological fluid behaviors.

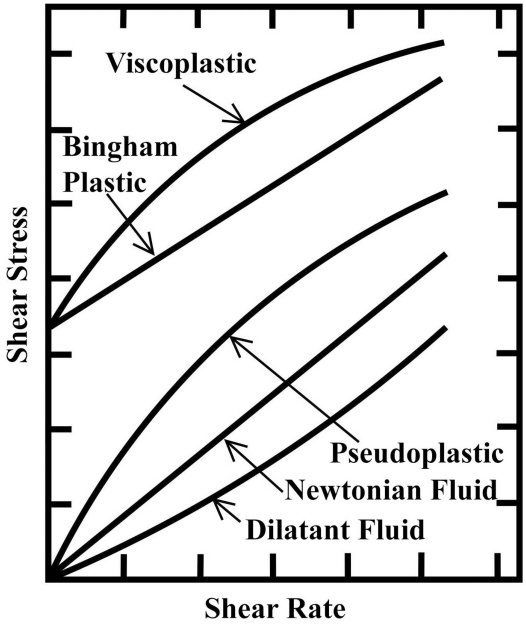

Source: CHHABRA (2010).

For example, Bingham fluid is different from Newtonian fluid because it presents a yield stress, which is required for the initial deformation of the fluid. When the shear rate increases, the apparent viscosity decreases, and the fluid is referred to as pseudoplastic (JABBARI et al., 2016). The inverse behavior is called dilatant. This is defined by an apparent viscosity increasing with the addition of the shear rate (CHHABRA, 2010). In both cases, the variation of the apparent viscosity as a function of the shear rate provides parameters of great interest. The pseudoplastic behavior can be caused by several factors such as the physical and chemical characteristics of the particles, as well as the concentration, interaction, dispersant, shaping, molecular weight and the shape of the particles (JABBARI et al., 2016).

In advanced ceramics processes like tape casting, pseudoplastic behavior is desirable to produce homogeneous tapes (JABBARI et al., 2016). When the suspensions contain particles with larger surface area, they become more susceptible to surface phenomena, which may lead to agglomeration (HOTZA; GREIL, 1995). The dilating behavior is related

to highly concentrated suspensions, due to the proximity of the particles. When at low shear rates, the flow is not hindered, the rate increasing is accompanied by the increasing in the difficulty of flow. Thus, some factors such as particle size distribution, repulsion and roughness forces may favor this rheological behavior (STUDART et al., 2006a).

2.2.1.1 Interaction between Particles

The strength of ceramic materials is limited by the presence of cracks and defects. These imperfections are usually caused by clusters resulting from the early stages of processing, leading to non-homogeneous packaging and leaving void spaces after sintering. An effective strategy for minimizing the number of agglomerates and homogenizing the powder is to use a dispersant in order to keep the particles dispersed in the liquid as a suspension (MISTLER; TWINAME, 2000).

Since the density of the solid particles is greater than that of the liquid, they tend to sediment. The forces acting on the particles help to understand how the stability of the suspension occurs. These can be either attractive or repulsive (MORENO; AGUILAR; HOTZA, 2012). When repulsive, the particles remain separated. However, when the forces are attractive, the formation of agglomerates occurs and the probability of sedimentation increases (RICHERSON, 2012).

The forces that act between particles determine their behavior and are called surface forces and body forces. These forces affect the stability and the rheology of the suspension (HOTZA, 1997).

2.2.1.2 Surface Forces

Also known as interatomic forces, surface forces can be classified as Coulomb and Van der Waals forces (KINGERY, 1977). The Van der Waals force is inversely proportional to the distance between the atoms. If all the atoms in the ceramic body are added together, the range of force increases significantly. However, the atoms closest to the surface of the body are those that predominantly increases (REED, 1995). The Coulomb interactions increases between charges normally encountered on the surface of the material (HOTZA; GREIL, 1995).

For instance, body forces act throughout the body and it is related with gravity, magnetic and electric fields. It contrasts with contact forces when exerted to the surface of the material

2.2.2 SLURRY COMPOSITION

The additives cover a very broad class of materials, usually organics. These materials are used as auxiliaries in the processing of ceramic materials (HOTZA; GREIL, 1995). They are extremely important in this process because they improve the plasticity and increase the green resistance of the material (REED, 1995).

The main additives used in the tape casting technique will be discussed below.

2.2.2.1 Binder

Generally, binders are polymer molecules that are adsorbed between ceramic particles acting like a bridge providing interparticle flocculation. These additives may provide several different functions to the ceramic body. It may improve the wetting of the particles which significantly increase the apparent viscosity. At green ceramic bodies the binder improves the plasticity and the green strength (REED, 1995). When the slurry has a high concentration of powder, a high molecular weight binder is required due to appropriate strength, pseudoplasticity and apparent viscosity (KINGERY, 1977). A critical step related to binders is their combustion. When burned in air, for instance, sodium carboxymethylcellulose (NaCMC) and some natural gums leave contaminating inorganic residues containing $K^{+,}$ P^{+} and Na^{+} ions, among others (NAYAK et al., 2011). When in an inert or reducing atmosphere, most of the binders leave some carbonaceous remnants. On the other hand, acrylic resins have complete combustion (HOTZA; GREIL, 1995).

Usually, a workable system is produced by using only one binder. There are any types of binders frequently used in tape casting process such as waxes, resins, gels and hydraulic cements. Polymers such as PEG (ALBANO; GARRIDO, 2006), latex (ALBANO et al., 2008) and acrylic resins (MORENO; AGUILAR; HOTZA, 2012) are mostly used in aqueous systems.

2.2.2.2 Plasticizer and Lubricants

Plasticizers are organic substances that have low molecular weight. After the drying process both the binder and the plasticizer are mixed. The plasticizer breaks down the bonds of the binder molecules, increasing the flexibility and workability of the material (HOTZA, 1997). Lubricants are generally composed of waxes or oils soluble in water and are intended to favor sliding between the particles (MISTLER; TWINAME, 2000).

2.2.2.3 Dispersant

Dispersant, also called deflocculant, wetting agent or surfactant basically coats the ceramics particles and keeps them apart, making the suspension stable due to steric and electrostatic repulsion (JABBARI et al., 2016).

In the processing of ceramic materials, the particles must be dispersed into a liquid allowing the homogenization and mixing of different particles. For accomplishing the dispersion of inorganic particle in the suspension, it is necessary to measure the isoelectric point of the solution to check when the suspension becomes unstable (JABBARI et al., 2016). Dispersions usually require a mechanical power to break through existing aggregates.

Due to the tendency of the particles to agglomerate, it is necessary to mix the powder with a liquid, using dispersing additives to stabilize the suspension and avoid agglomeration (PUJALA, 2014).

The dispersants are generally based on three different stabilizing mechanisms: steric, electrostatic and electrosteric. Particle agglomeration is associated with the Van de Waals force, with a potential attraction energy value (U_A).

To achieve a good dispersion, it is necessary to compensate the forces of attraction with repulsive forces, modifying the original agglomeration rate. This can be accomplished by mechanisms of stabilization which involve adsorption of polymers with long chains, increasing steric hindrance and development of electric charges on the particle surface by adsorption of molecules with ionizable groups (HOTZA; GREIL, 1995; OLIVEIRA; TOREM, 2001; NISHIHORA et al., 2018).

The most frequently used dispersants for aqueous tape casting are polyelectrolytes such as sodium salts of cellulose derivatives (NaCMC)

and ammonium salts NH_4PMA and NH_4PA (GOULART; SOUZA, 2017).

2.2.2.4 Surfactant

The molecules present in a surfactant tend to adsorb on the surface for their polar and nonpolar characteristics. The surfactants have a polar head which is soluble in water and a nonpolar tail, which is not soluble in water (REED, 1995).

When in solution, the surfactant forms micelles, Fig. 6. However, when a particle is present in the medium, its hydrophilic part can adsorb on the particle surface when the surface is polar and with the hydrophobic part if the surface is nonpolar (MISTLER; TWINAME, 2000).

Fig. 6 - Different behaviors of surfactant in solution in polar and nonpolar areas.

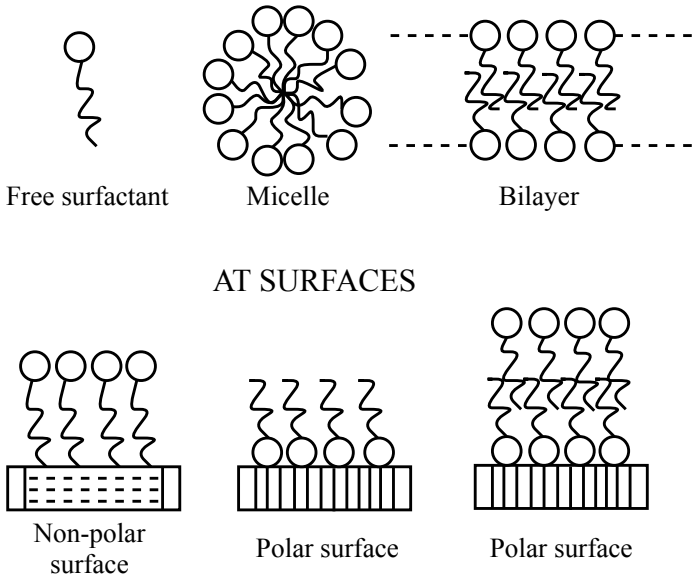

Source: Adapted from (TERPSTRA, 1995).

When enough surfactant is dissolved in water, it must adsorb the polar forming layers and exposing the non-polar ionic groups to the aqueous phase. This mechanism removes the hydrophobic interaction and promotes repulsion through an electric double layer, stabilizing the suspension. This same ionic surfactant may act inversely if a stable medium of hydrophilic particles of opposite polarity occurs. In this case, with its ionic group of the head adsorbed, it neutralizes the charge of the surface and makes the surface hydrophobic, agglomerating the particles (MISTLER; TWINAME, 2000). An adsorbed surfactant can affect various forces between surfaces, such as Van der Waals. Moreover, a limited thickness of adsorbed monolayers prevents the surface particles from approaching the region where the Van de Waals force is stronger. This effect is known as steric stabilization which keeps the particles moderately separated (REED, 1995).

Usually, there are three classes of surfactants, i) nonionic, ii) anionic and iii) cationic. The most frequently used surfactants for aqueous tape casting are ethoxylated nonyphenol, sodium stearate, dodecyltrimethylammonium chloride and diethanolamide (REED, 1995).

2.2.2.5 Anti-Foaming agent

An anti-foaming agent should reduce the surface tension of the foaming solution, increase the film elasticity and removing bubbles. Aqueous foaming additive may contain a surfactant that makes the particles hydrophobic and reduces the surface tension. Tall oil, polypropylene glycol, sodium alkyl and silicone emulsions are effective as aqueous anti-foaming agents (LIU; CHEN, 2014).

2.2.2.6 Sacrificial Pore Former

Pore former agents are incorporated in suspensions leaving empty spaces after burning, generating porosity. (STUDART et al., 2006b; HOOG et al., 2018). After the heat treatment, the ceramic powder is the only component remaining in the material (Fig. 7).

Although all organic components of the tape can be treated as pore formers, it is necessary to optimize the suspension (NISHIHORA et al., 2018b) since some components cannot exceed a limit value so that the

tape can be processed. Porous former agents are generally polymers with different particle sizes in the micrometer range (STUDART et al., 2006b).

Among the polymers that can be used as pore formers, poly (methyl methacrylate) (PMMA) is one of the most used to produce highly controllable pores by the sacrificial method (BOARO et al., 2003; SANTA CRUZ; SPINO; GRATHWOHL, 2008). The size of the PMMA microspheres can range from a few nanometers to values around 100 µm (STUDART et al., 2006b). These values depend on the degree of polymerization which is linked to the average molecular weight of the polymer (JABBARI et al., 2016; NISHIHORA et al., 2018b; STUDART et al., 2006b).

Fig. 7 - Scheme of sacrificial pore formers method.

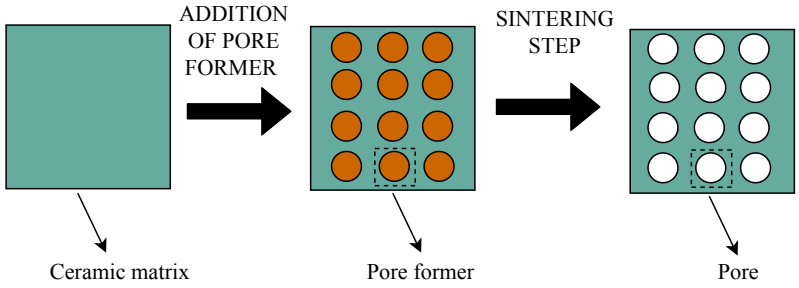

Source: Elaborated by the author (2019).

2.3 SURFACE FUNCTIONALIZATION

The functionalization of the ceramic surface brings a wide range of possibilities to promote new functionalities to the ceramics materials, to increase its efficiency and applicability (ANWANDER et al., 2000; TRECCANI et al., 2013; ZHOU et al., 2007). The fundamental concepts, although much investigated today, date back several decades. The specific strategy is related to the intended application. These strategies are classically divided into three main categories: physical, chemical and biological (TRECCANI et al., 2013). Each corresponds to a different technique used in surface modification. The combination of more than one functionalization technique to the material can be used to confer several functionalities to the same material (KOZLOVA et al., 2012; NAMGUNG et al., 2011).

Chemical functionalization consists mainly of changing the composition and charge on the surface of the material. The most popular methods for chemical modification are ionic bombardment (HOWLETT et al., 1994), slurry-based techniques (MIAO et al., 2007), acid or alkaline treatment (ZHAO; LIU; DING, 2005) and the fixation of organic functional groups to the surface of the material, both by physisorption and by covalent bonding (NEOUZE; SCHUBERT, 2008).

The functionalization of inorganic substrates via anchoring of organic molecules to the surface is an effective way to adjust the properties of the surface. For ceramic materials, surface modification is usually carried out by silanization, as shown in Fig. 8 (KOHLER; FRYXELL; ZHANG, 2004; CAUDA; SCHLOSSBAUER; BEIN, 2010; KROLL et al., 2010; KROLL et al., 2012; BARTELS et al., 2016). The method has become feasible because it can be carried out at moderate temperatures and no particular conditions or expensive equipment is necessary. Moreover, it is applicable to any type of material and support, such as colloidal particles (HADDADA et al., 2013), planar surfaces (SCHICKLE et al., 2012) and porous membranes (BARTELS et al., 2016; HOOG et al., 2018; JAVAID et al., 2006).

To employ the technique effectively, the silane molecules must be first activated by hydrolysis. Thereafter, the condensation reactions occur between the Si-OH groups of the silanol and the OH groups on the surface. This leads to the formation of a stable bond with the surface and the release of free alcohols as side products.

Fig. 8 - Silanization of ceramic surfaces.

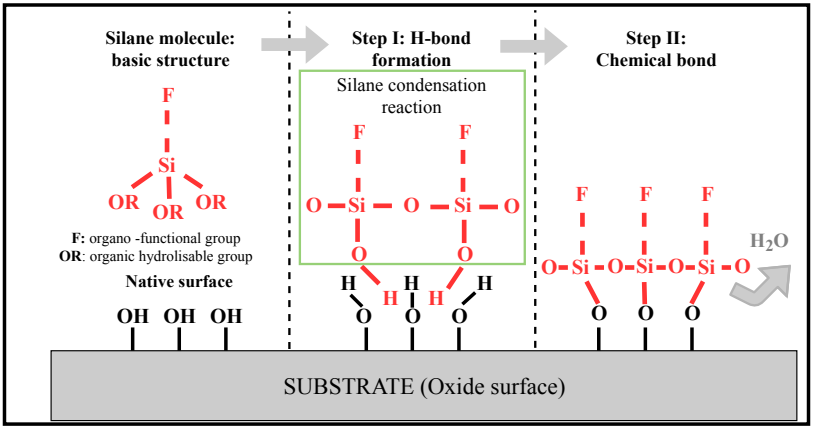

Source: Adapted from TRECCANI et al. (2013).

Silanization can be performed in both aqueous and organic solvents. Generally, silanization in aqueous media generates a more uniform coverage and a thinner silane layer in the substrate (TRECCANI et al., 2013). Due to the high variety of studies using surface modification, most of these have employed aminosilanes, in particular, (3-aminopropyltriethoxysilane) so-called APTES (HOWARTER; YOUNGBLOOD, 2006; KROLL et al., 2010; BARTELS et al., 2016).

The popularity of APTES, Fig. 9, is related to its intrinsic chemical properties (TRECCANI et al., 2013). The NH_2 groups present in these compounds promotes adhesion in glass-resin composites as well as promote and control biomolecular adhesion (MEDER et al., 2012), enzymatic stability (LI et al., 2010) and increase in hydrophilic properties (HOWARTER; YOUNGBLOOD, 2006).

Fig. 9 - Chemical structure of 3-aminopropyltriethoxysilane (APTES).

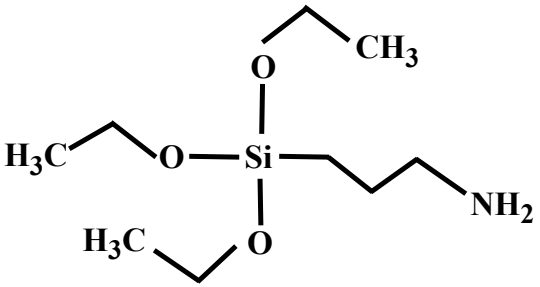

Source: Elaborated by the author (2019).

Due to the intrinsic properties of APTES and the gap in the literature related to its use in microfiltration field, the aim of this study is to contribute in the developing of materials with new functionalities which currently is not well-known and deserve more attention.

It could be noted that even though several works using zirconia membranes for virus, bacteria filtration and oil/water separation were published, only few studies (BARTELS et al., 2016; HOWARTER; YOUNGBLOOD, 2006; KROLL et al., 2010; MCCOOL; DESISTO, 2005) present increased permeability by increasing hydrophilicity by anchoring functional groups on the surface of the ceramic material.

3 MATERIALS AND METHODS

3.1 MATERIALS

To produce porous ceramic tapes, zirconia powder stabilized with 8 mol% yttria (8YSZ, cubic zirconia, — Innovnano with 99.9% purity, average particle size 450 nm and specific surface 28.53 m^2/g was used. A commercial solution of ammonium polyacrylate (Darvan 821 A, Vanderbilt) was used as dispersant and a styrene-acrylic latex emulsion was used as the binder (Mowilith LDM 6138, Clariant). Poly(methyl methacrylate) (PMMA) with a mean particle size of 5 μm, M_w= 1.4 $x10^6$ g/mol and 1.8553 m^2/g specific surface area was used as a pore-forming agent, diethanolamine was used as surfactant and an aqueous-silicone emulsion (Y-30 Emulsion, Sigma Aldrich) was used as anti-foaming agent.

3.2 SLURRY PREPARATION

Aqueous slips were prepared by de-agglomeration of 8YSZ and PMMA powders in de-ionized water with 1 wt% dispersant by ball milling for 24 h. The binder, antifoam, and solvent were added and the slurry was mixed by ball milling for 30 min. The slurry was then left to rest for 2 h to remove air bubbles. The compositions are shown in Table 2. The compositions for the slurries were optimized from a range of ceramic powder compositions (20 to 55 wt%) and established based on both additive supplier application data sheets, the previous experience of the group and processability (MORENO; AGUILAR; HOTZA, 2012).

Table 2 – Slurry compositions.

Component	YSZ_PF (wt%)	YSZ_NPF (wt%)
YSZ	24	30
PMMA	6	-
Deionized water	52	52
Dispersant	1	1
Binder	15	15
Surfactant	1.5	1.5
Anti-foam	0.5	0.5

YSZ_PF: pore former, YSZ_NPF: no pore former.
Source: Elaborated by the author (2019).

3.3 TAPE CASTING

The slips were cast with a tape caster machine (CC-1200, Mistler) onto a moving support film of polyethylene terephthalate (PET, mylar) with a fine coating of silicone layer (G10JRM, Mistler). The casting speed was constant and set at 1 mm/s and the gap between the blade and the carrier was adjusted manually. In order to obtain a final tape thickness of 0.2 to 0.3 mm after drying a second cast above the green body was carried out manually.

3.4 DRYING

The drying parameters of the tapes were defined by an experimental design combining three different temperatures (20 °C, 35 °C and 50 °C) and relative humidity (55%, 70% and 85%) using a climate chamber (Model BD 56, Binder). The temperature and the relative humidity that did not cause cracks, defects or warping in the green tapes were 20 °C and 85% and therefore used in all further assays.

3.5 SINTERING

For firing and sintering steps, the tapes were cut in 2×2 cm samples and placed on alumina plate and covered with alumina slides to prevent warping. The elimination of the solvent and the burning out of polymer additives was obtained by slow heating (1 °C/min) up to the target temperatures, which were 1300, 1400 and 1500 °C, respectively, with 2 h

as dwell time at these target temperatures. The cooling step was fixed in 5 h.

3.6 CHARACTERIZATION TECHNIQUES

3.6.1 Powder characterization

Yttria-stabilized zirconia and PMMA powders were first characterized using a scanning electron microscope (SEM, Camscan, Series 2, Obducat CamScan) at 20 kV after sputtering the samples with gold to assess morphology and particle size. Yttrium-stabilized zirconia (YSZ) particle size was determined by Dynamic light scattering (DLS, Malvern, ZetaSizer/Nanosizer). The PMMA polymer particle size was measured in an acoustic and electroacoustic spectrometer (Model DT-1202).

3.6.2 Rheometry

The rheological behavior of the slurry was measured in a rotational rheometer (Kinexus Pro+, Essentials, Malvern) with a shear rate geometry at room temperature. The rheogram of the slurry was made at a shear rate of 0.01 to 500 s^{-1}.

3.6.3 Zeta potential

Zeta potential of the dispersion of YSZ in deionized water was measured at various pH values. YSZ was dispersed in water at 1 wt% using dispersant (Darvan 821 A, R. T. Vanderbilt) at 1 wt% related to the powder. and sonicated for 10 min at 10 W. The measurements were carried out in a zeta potential and particle size meter based on acoustic and electroacoustic spectrometer (DT 1200, Dispersion Technology). For titration, KOH and HCl (1 mol. L^{-1}) were used.

3.6.4 Microstructure

The membranes microstructure was observed in a scanning electron microscope (SEM, Camscan, Series 2, Obducat CamScan) at 20

kV after sputtering the samples with gold. A dedicated software (Image J, NIH)) was applied at the images to measure the average pore size. (SCHNEIDER; RASBAND; ELICEIRI, 2012). After functionalization, microstructural observations were carried out in a scanning electron microscopy (SEM) with electron dispersion X-ray (EDX) for chemical analysis using a ZEISS Supra 40 SEM (ZEISS, Oberkochen, Germany with acceleration voltage of 0.5 kV).

3.6.5 Pore size distribution and porosity

The pore size distribution (micro-meso-macro pore ranges from 0.01 to 100 μm) and open porosity were determined using mercury intrusion porosimetry (Pascal 140/440, Porotec).

3.6.6 Nitrogen adsorption isotherms and specific surface area

The specific surface area (SSA) was determined by nitrogen adsorption and desorption isotherms measured at 77 K (Belsorp-Max, Bel Japan).

3.6.7 Surface characteristics

Hydrophilicity and hydrophobicity characteristics were studied by water and n-heptane vapor adsorption, which were carried out by exposing ~0.5 g of the sample as a powder to the water and heptane vapor in a closed vessel for 24 h at 25 °C. Vapor adsorption, expressed in $mmol.m^2$ was determined by change in sample weight. The procedure was adopted following the method previously proposed by the group.

3.7 FUNCTIONALIZATION

With the objective to modify the surface characteristics of ZrO_2 membranes, the surface functionalization was carried out following a method proposed elsewhere (BARTELS et al., 2016):

Step 1– Acidic hydroxylation of the surface using Piranha solution (97% H_2SO_4: 35% H_2O_2, 3:1 v/v). The YSZ membrane samples were immersed in the solution at room temperature (RT) for 30 min. Afterwards the membranes were rinsed with water until the effluents achieved a neutral pH followed by drying at 70 °C for 16 h.
Step 2– The samples (7 mm^2) were immersed in a 0.2 mol. L^{-1} solution of (3-Aminopropyl) triethoxysilane (APTES) in a falcon tube (15 mL) and incubated in a rotary shaker at 150 rpm and 65 °C for 24 h.
Step 3– After this procedure, the membranes were washed with deionized water at least 5 times for 2 minutes until the water reached neutral pH.
Step 4– The membranes were kept inside the open falcon tubes and then dried at 70 °C for 24 h. The tubes were covered with lint-free paper to avoid contamination.

3.8 PERMEABILITY TESTS

The water permeation test measures were carried out in a dead-end permeation device depicted in Fig. 10. The equipment consists of a feed tank (200 mL), a membrane module and a valve that controls the pressure inside the tank monitored by a manometer.

Measurement of permeability is usually performed on linear, mostly cylindrically shaped, so-called “core” samples. The experiment was arranged to have vertical flow through the sample.

Fig. 10 - Scheme of permeability device used in the water flux tests.

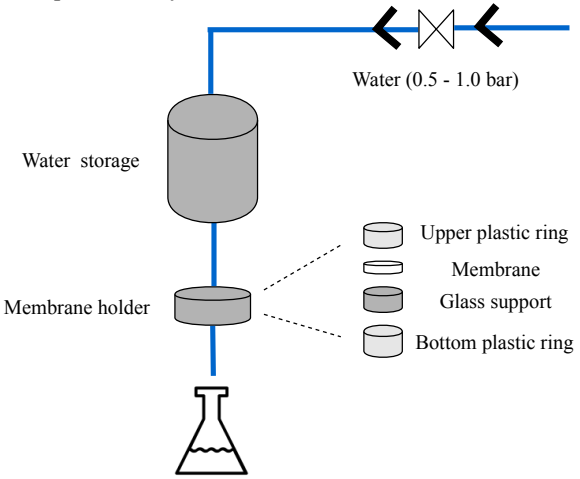

Source: Elaborated by the author (2019).

Considering the permeate flux as a classical filtration theory described by first Fick's law from transport phenomena, the permeate flux was analyzed considering the equation (1).

$$J = \frac{dV}{dt} \times \frac{1}{A_m} \tag{1}$$

where J is the transient permeate flux, dV is the differential volume, dt is the differential time and A_m is the effective membrane surface area.

Pressure was varied from 0.5 to 1.0 bar and temperature was kept constant at 25 °C. Three membranes of each composition were tested.

4 RESULTS AND DISCUSSION

4.1 CHARACTERIZATION OF POWDER AND SUSPENSION

4.1.1 Particle size

Yttria-stabilized zirconia (YSZ) particle size determined by DLS was approximately 433 ± 3 nm, which is within the range reported by the manufacturer data (450 nm).

The PMMA was previously prepared by a standard emulsion method (ARORA et al., 2010). An average PMMA particle size of 5 μm with an irregular particle size distribution was obtained.

Fig. 11 shows SEM images of the YSZ (left) and PMMA (right) powders. The powders, due to the small particle size, form agglomerates during sample preparation. Thus, it was not possible to confirm the average size data obtained by other techniques.

Fig. 11 - SEM micrographs of the starting powders, zirconia 8YSZ (left) and PMMA (right).

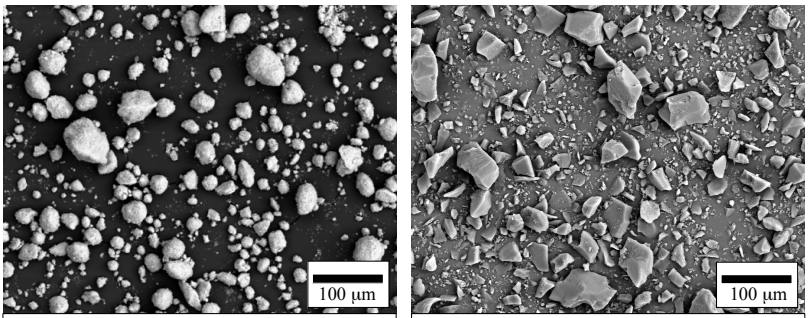

Zirconia 8YSZ (432,7 nm) | Polymer PMMA (3,41 μm)

Source: Elaborated by the author (2019).

4.1.2 Rheometry

Fig. 12 presents the shear stress vs. shear rate curve of the different slurry compositions. The samples were labeled as YSZ_PF and YSZ_NPF for the sample with pore former and without pore former, respectively. Both curves showed a pseudoplastic behavior, which is desirable in the slips for tape casting process. Slurries with this behavior show a decrease in the viscosity with the increase of the shear rate, which means that the viscosity is maximal at rest or without any shear rate (MORENO; AGUILAR; HOTZA, 2012).

In the tape casting process, it is important that the slurry viscosity decreases under shear forces generated when the slip is flowing through the blade, so that it offers low resistance to flow. After passing through the blade the shear rate returns to zero and the viscosity increases again (ALBANO; GARRIDO, 2006; MISTLER; TWINAME, 2000). This behavior is essential to maintain the tape shape constant, especially its thickness, during the drying step (REED, 1995).

Fig. 12 - Shear rate vs. shear stress slurries with (YSZ_PF) and without (YSZ_NPF) pore former.

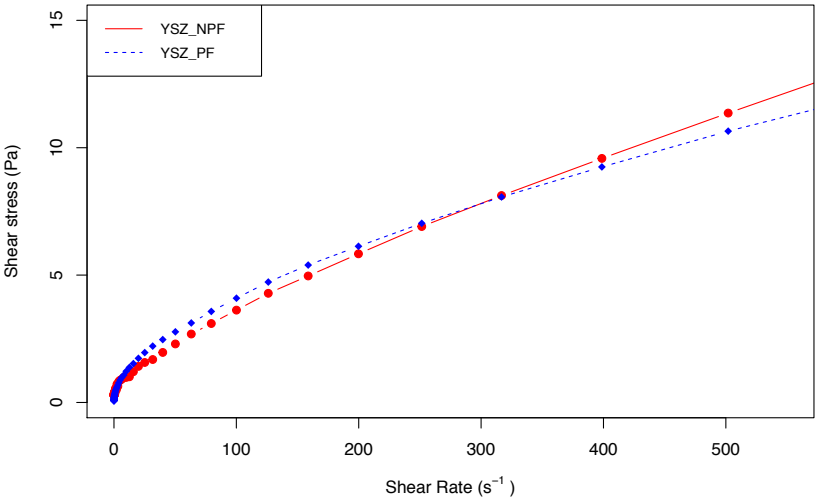

Source: Elaborated by the author (2019).

4.1.3 Zeta potential

The zeta potential vs. pH of the YSZ with dispersant is shown in Fig. 13. The slurry presented a zeta potential in a range between 60 and -50 mV. The isoelectric point (IEP) was found at pH 7.25. Usually, the addition of dispersant reduces the IEP and makes the slurry stable at lower pH values. It is widely known that the higher the zeta potential is, the better the slurry stability. Zeta potential module higher than 30 mV corresponds to a stable slip (HOTZA; GREIL, 1995). Stable slurries promote the manufacturing of homogeneous ceramic tapes with great green resistance and fewer defects (REED, 1995). The optimal pH for the stabilization of the slurry during the process is between 4 and 6 or between 8 and 10 where the highest zeta potential value was found.

Fig. 13 - Zeta potential vs. pH of 1 wt% YSZ powder in water with dispersant (Darvan 821) at 1 wt% related to the powder.

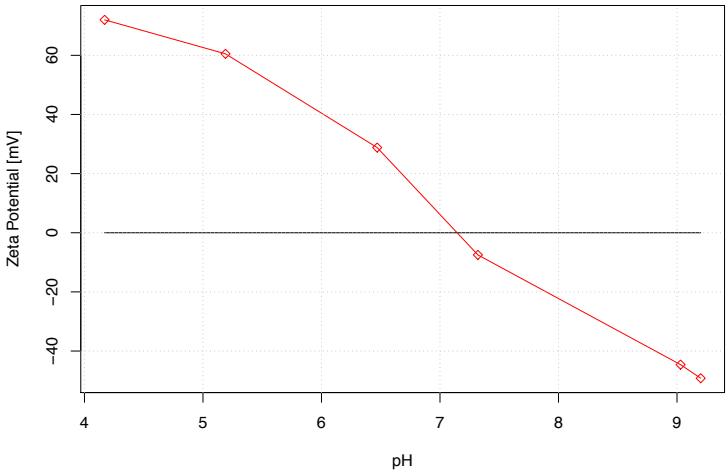

Source: Elaborated by the author (2019).

4.2 MEMBRANE STRUCTURAL CHARACTERIZATION

4.2.1 Membrane morphology

Fig. 14 shows the cross-section and top surface from the SEM of the sintered tapes with and without pore former (YSZ_PF and YSZ_NPF, respectively). The images were treated in ImageJ (SCHNEIDER; RASBAND; ELICEIRI, 2012) software to estimate the surface pore size on the structure.

As it can be seen in Fig. 14 (a) - (d) the cross section of the tapes showed that the lamination was carried out successfully, i.e., no cracks or delamination was detected. The tapes presented thickness values between 220 and 224 μm for the YSZ_NPF samples and around 200 μm for the YSZ_PF membranes. An anisotropic sintering shrinkage (~8%) parallel and perpendicular to the casting direction was observed. This behavior was also reported by Albano and Garrido (2006) and it is common during the sintering step.

Figures 14 (e) - (h) show the top surface of the tapes. A small uniform pore size distribution with an average pore size diameter of 0.3 μm was observed in Fig. 14 (e) (YSZ_NPF_1300). However, in Fig. 14 (f) (YSZ_PF_1300), an increasing of average pore size to 0.5 μm was noticed when the pore former was added at the tape sintered at 1300 °C. This behavior is expected since the addition of pore former leave blank spaces after sintering.

Fig. 14 (g) (YSZ_PF_1400) shows the SEM micrograph of the membrane sintered at 1400 °C, and larger average pore size was observed, with values around 1.4 μm. This behavior can be related to the higher interconnection between pores during the structure accommodation caused by the phase transition, resulting in bigger cavities or channels (NISHIHORA et al., 2018a).

The pore coalescence during sintering might contribute to the enlargement of the pores in the matrix. This fact can be easily noticed at 1400 °C. On the other hand, the tapes sintered at 1500 °C (Fig. 14 (h), (YSZ_PF_1500)) showed an average pore size of 0.7 μm. The reason for this pore size decreasing might be related to the structure accommodation during phase transition (FLETCHER ANDREW, 1993).

Figures 14 (e) - (h) show irregular shaped pores, and this can be justified by the shape and size of the PMMA particles used as sacrificial

pore former. This perspective was previously observed by Albano et al. (2008).

The addition of PMMA helped to avoid the high densification. The PMMA particles have an average particle size of 5 μm, but the pores generated for these particles suffer coalescence during sintering (BOARO et al., 2003). The pores could also coalesce during sintering, so that the pore size increased with addition of PMMA. The bigger the pore size and the surface area, the lower the driving force for sintering and shrinkage (ALBANO et al., 2009).

Fig. 14 - Cross section and top surface microstructures from different sintering temperatures (a) YSZ_NPF_1300, (b) YSZ_PF_1300, (c) YSZ_PF_1400 and (d) YSZ_PF_1500 and top surface (e) YSZ_NPF_1300, (f) YSZ_PF_1300, (g) YSZ_PF_1400 and (h) YSZ_PF_1500.

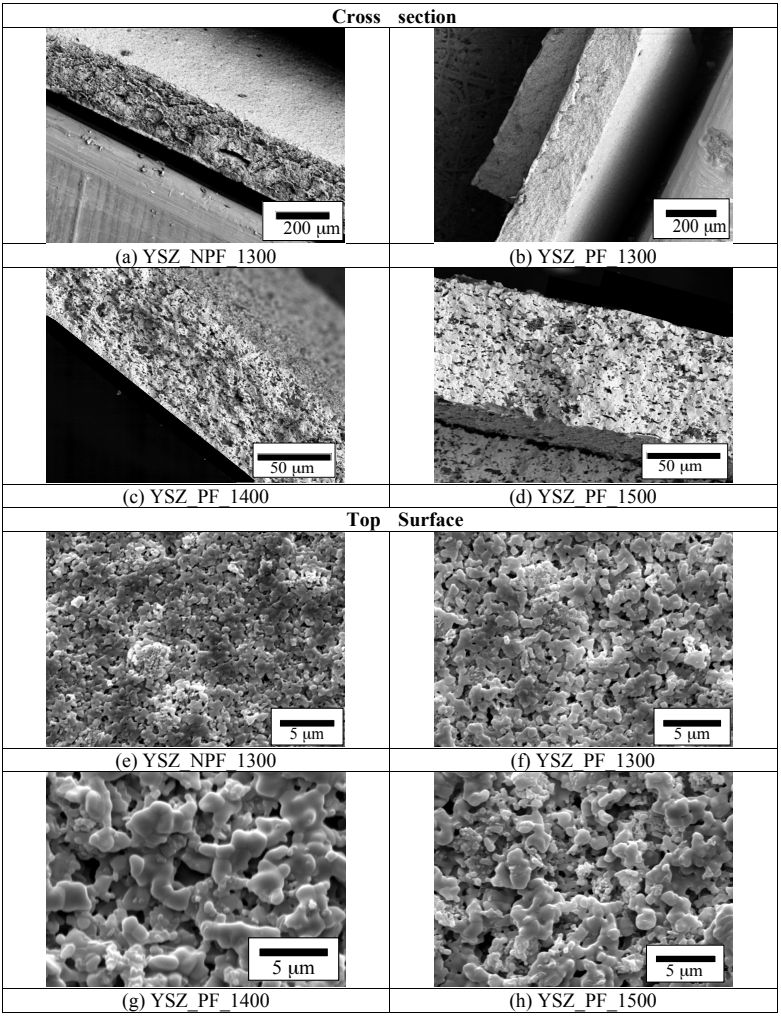

Source: Elaborated by the author (2019).

4.2.2 Pore size distribution and porosity

Fig. 15 shows the results obtained by mercury intrusion porosimetry for all the sintered tapes. The open porosity varies in a range between 27% and 51% according to the use of PMMA and the sintering temperature. The PMMA content had a positive effect in the open porosity.

Fig. 15 - Pore size distribution and open porosity of the membranes samples in different temperatures.

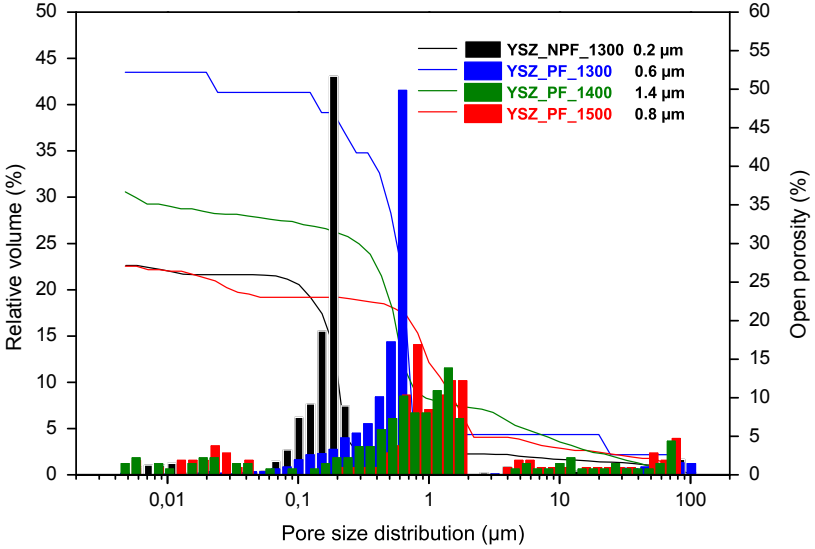

Source: Elaborated by the author (2019).

The pore diameter can be controlled first by altering the sacrificial pore former and sintering temperature. The results obtained by Hg intrusion showed a pore range between 0.01 and 100 µm. The lower values (0.01 µm) correspond to the binders burned out during sintering. On the other hand, higher values in a range of 100 µm are probably related to cracks and defects presented in the membranes. The YSZ_PF_1400 and YSZ_PF_1500 membrane samples presented a bimodal pore size distribution with an average pore size of 1.4 µm and 0.8 µm, respectively. Comparable values were extracted from the ImageJ software. This fact indicates the collapse of the small pores. For the lower temperature

samples, YSZ_NPF_1300 and YSZ_PF_1300, bimodal distributions were obtained with average values of 0.2 and 0.6 μm, respectively. Excluding the low fractions of large pores, all the samples showed a pore distribution in a range between 0.1-1.5 μm, which suggests a symmetric pore shape. In symmetric membranes, which are suitable for microfiltration, the thickness of the entire membrane membrane determines the flux passing through it.

4.2.3 Nitrogen adsorption isotherms

Nitrogen adsorption isotherms and specific surface area (SSA) of the sintered membranes were investigated to determine the influence of the sintering time in the microstructure. Table 3 presents the specific surface area and isotherm type obtained from the nitrogen adsorption isotherms for the different samples. The membrane sintered at 1300 °C without PMMA achieved a specific surface area of 1.24 $m^2 \cdot g^{-1}$ (YSZ_NPF_1300). This SSA is increased to around 1.74 $m^2 \cdot g^{-1}$ (YSZ_PF_1300) with the addition of 6 wt% pore former. On the other hand, for the sample sintered at 1400 °C, the SSA showed considerable reduction to 0.85 $m^2 \cdot g^{-1}$ (YSZ_PF_1400). Further increase in sintering, at 1500 °C, caused a decrease in SSA to 0.24 $m^2 \cdot g^{-1}$ (YSZ_PF_1500). Comparable SSA values were reported in the literature for monoclinic zirconia (EDER; EDER; KRAMER, 2014) and it's expected for ZrO_2 materials.

All the isotherms can be classified as type II (Appendix A), which is typical for macroporous solids showing macropores filling but no multilayer adsorption (KELLER; STAUDT, 2005).

Table 3 - Specific BET surface areas and isotherm types of four samples.

Sample	SSA ($m^2 \cdot g^{-1}$)	Isotherm type
YSZ_NPF_1300	1.24	II
YSZ_PF_1300	1.74	II
YSZ_PF_1400	0.85	II
YSZ_PF_1500	0.24	II

Source: Elaborated by the author (2019).

4.2.4 Microstructure of the samples before and after functionalization

Fig. 16 shows EDX compositions measured before and after silanization, following the method previously proposed by Bartels et al., (2016).

Fig. 16 - SEM-EDX results of the control sample YSZ_PF_1300(a) and the three functionalized membranes YSZ_PF_1300_APTES(b), YSZ_PF_1400_APTES(c) and YSZ_PF_1500_APTES(d).

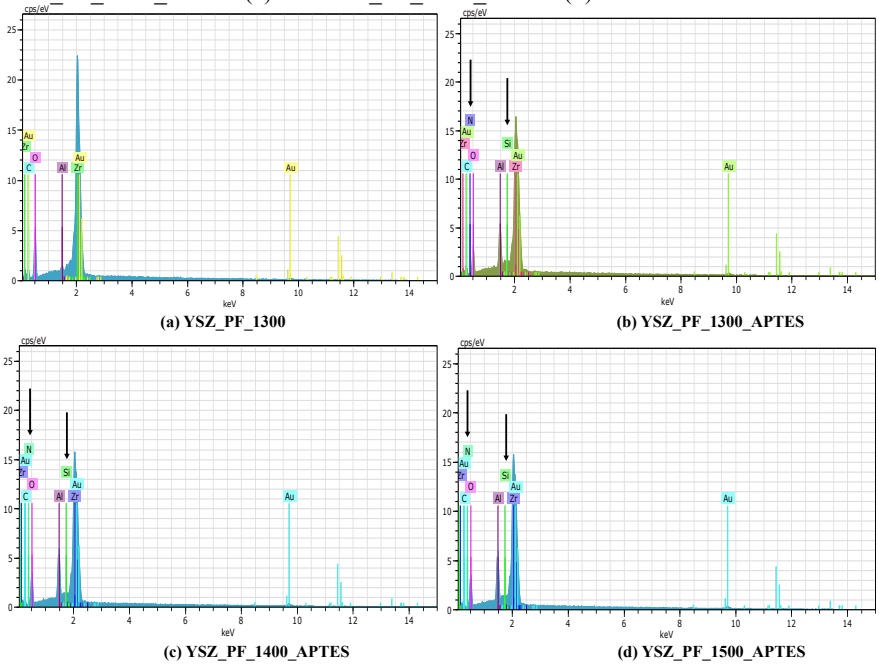

Source: Elaborated by the author (2019).

As expected, the YSZ_PF_1300 membrane (Fig. 16 (a)) did not show the presence of silicon (Si) and nitrogen (N) atoms present in APTES. All functionalized membranes, Figures 16 b, c and d a considerable amount of Si and N was detected, evidencing the success in APTES deposition on the membrane surface, as also shown in the literature (MCCOOL; DESISTO, 2005).

Carbon peaks were also present and may in turn, refer to the glue used to accommodate samples in the sample holder and carbon moiety of APTES. Oxygen peaks are attributed to the zirconium oxide membrane surface.
Therefore, it can be concluded that the functionalization occurred satisfactorily, promoting the anchoring of functional groups on the surface of the material.

Table 4 shows that the silicon content was higher compared to the nitrogen content in the samples. This can be explained by the higher molecular weight of silicon compared to nitrogen. However, the compositions remain essentially the same, suggesting that the amount of APTES deposited on the membranes surface was constant.

Table 4. EDX results of the (a) control sample, and the three functionalized membranes (b) YSZ_PF_1300_APTES, (c) YSZ_PF_1400_APTES and (d) YSZ_PF_1500_APTES.

	Composition (wt%)	
Sample	**Nitrogen (N)**	**Silicon (Si)**
YSZ_PF_1300	-	-
YSZ_PF_1300_APTES	0.38	1.78
YSZ_PF_1400_APTES	0.28	1.72
YSZ_PF_1500_APTES	0.27	1.75

4.2.5 Surface characteristic

The vapor adsorption of polar (water) and non-polar (n-heptane) solvents were carried out to determine the membrane surface properties, as displayed in Fig. 17. All the samples presented a hydrophilic behavior which is common for oxidic ceramics (RUDAKOVA et al., 2016). YSZ_NPF_1300 membranes tend to be more hydrophilic with sorption values of 0.65 mmol/m^2 and 0.28 mmol/m^2 of water and n-heptane, respectively. Water adsorption had a ratio 2.3 higher than n-heptane uptake. These values are comparable to the ones in the literature referring to zirconia oxidic membranes (RUDAKOVA et al., 2016; ZHU et al., 2014).

Regarding YSZ_PF_1300 membranes, sintered at the same temperature, but with the use of pore former in the slurry formulation, a hydrophilic surface was also obtained. The ratio of water to heptane uptake (w/h) was equal to 2.3. Suggesting that neither the porosity nor the pore size plays a role in the surface properties.

The average amount of water and n-heptane adsorbed by YSZ_PF_1400 was equal to 0.62 mmol/m^2 and 0.22 mmol/m^2, respectively, resulting in a w/h ratio of 2.7 times. Nevertheless, for the YSZ_PF_1500 membranes, values of 1.5340 mmol/m^2 and 0.5217 mmol/m^2 were obtained for water and n-heptane, respectively, representing an increment of 2.9 times in hydrophilicity.

An increasing hydrophilicity and hydrophobicity as a function of temperature was discussed elsewhere (Botha, P. J. et al. 1998), and related to the greater lattice parameter of the cubic crystalline structure in higher temperatures, which increases the interaction between oxygen atoms and H_2O and C_7H_{16} molecules, enhancing the vapor uptake.

Fig. 17 - Water and n-heptane vapor adsorption at 25 °C and ratio of maximum water/n-heptane adsorption for YSZ samples sintered at different temperatures.

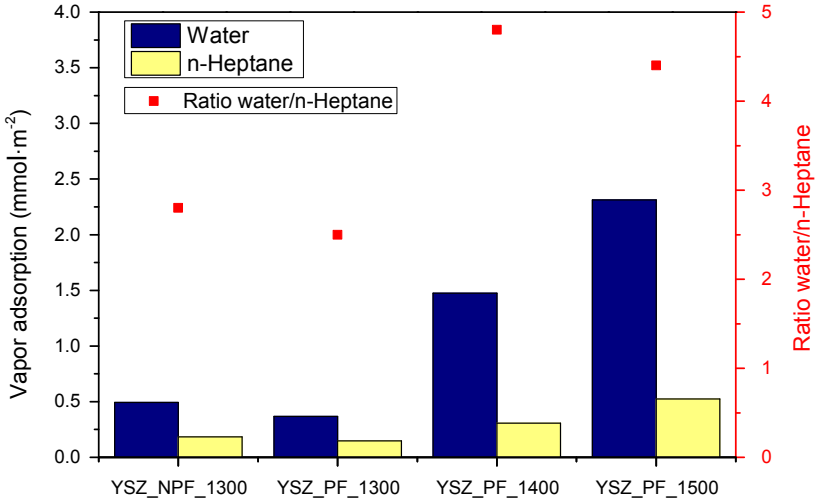

Source: Elaborated by the author (2019).

4.3 WATER PERMEABILITY

4.3.1 Non-functionalized membranes

The membrane performance was evaluated in a dead-end permeation device to measure the permeate flux before functionalization, Fig. 18, at three different working pressures (0.5, 0.75 and 1 bar).

Fig. 18 - Permeate flux performance of non-functionalized membranes at three different working pressures (0.5, 0.75 and 1.0 bar). Values above each set of bars for the water permeability calculated by the slope of permeate flux vs. transmembrane pressure linear fit.

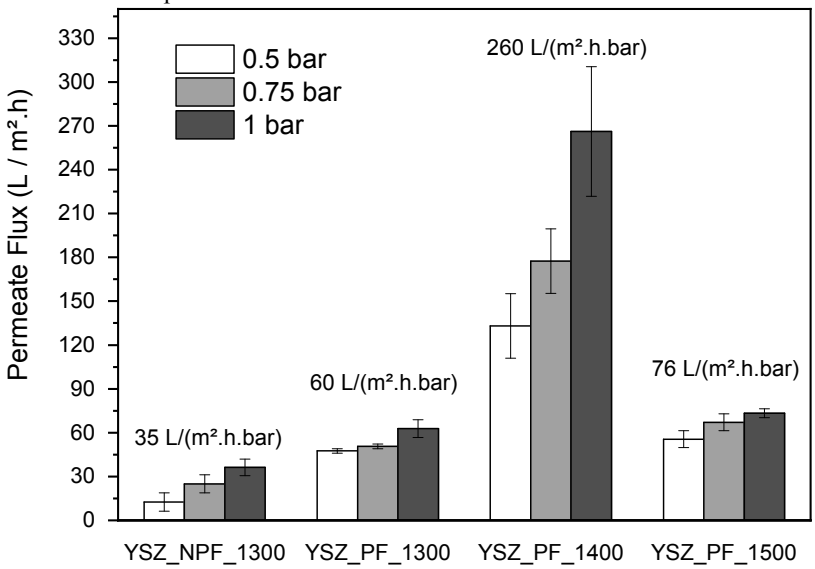

Source: Elaborated by the author (2019).

For the YSZ_NPF_1300 sample a low transient permeate flux at the three different pressures can be noticed. This result agrees with the porosity and the average pore size of the sample (27% and 0.2 μm). In contrast, the YSZ_PF_1300 sample showed a slight increase in the transient permeate flux, due to higher porosity (51%) and pore size (0.6 μm) when compared with the previous sample. The same trend is observed for samples YSZ_PF_1400. Comparable behaviors were

reported by Bouzerara et al. (2012) for zirconia microfiltration membranes manufactured by slip casting. The transient permeate flux of the YSZ_PF_1500 sample which has an average pore size of 0.8 μm and a porosity of 27% was similar to the two first samples (YSZ_NPF_1300 and YSZ_PF_1300).

It can be noticed that even though the porosity plays a role in the water permeability, the average pore size seems to have a stronger influence on the permeate flux. This behavior is also reported by previous studies, for instance in the dead-end microfiltration of yeast using alumina membranes (MAHESH KUMAR; ROY, 2008).

4.3.2 Functionalized membranes

After the functionalization procedure, the performance of the membranes was evaluated for comparison with the control membranes. The same parameters were considered and the transient flux was calculated. Fig. 19 displays the functionalized membranes performance in three different working pressures (0.5 bar, 0.75 bar and 1 bar).

Fig. 19 - Permeate flux tests of the functionalized membranes (YSZ_PF_1300), (YSZ_PF_1400) and (YSZ_PF_1500) as a function of 3 different working pressures. Values above each set of bars stand for the water permeability calculated by the slope of permeate flux vs. transmembrane pressure linear fit.

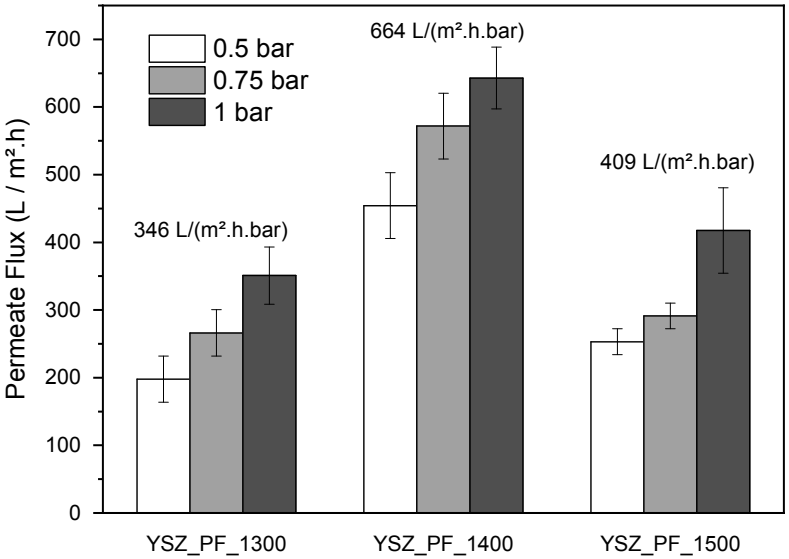

Source: Elaborated by the author (2019).

The YSZ_NPF_1300 sample was not evaluated due to the average pore size, which was very small (0.2 μm) and could even decrease after functionalization, making the sample unable to be used in microfiltration process. The decreasing of pores size after surface functionalization was also observed by Mccool and Desisto, (2005) for silica membranes.

The samples sintered at 1300 °C and 1500 °C with pore former (YSZ_PF_1300, YSZ_PF_1500) showed fluxes 5 times higher when compared with the same samples before functionalization. Nevertheless, the YSZ_PF_1400 sample showed the highest water permeate flux, 3 times higher compared with the non-functionalized membrane. This behavior can be explained by the high average pore size as well as the higher porosity of YSZ_PF_1400 membrane when compared with the other two membranes (YSZ_PF_1300 and YSZ_PF_1500).

When the surface is modified with APTES, amino groups (NH_2) are attached on the membrane surface. These groups increase the interaction with water and facilitate water permeation through the pores.

This effect was also observed elsewhere (BOUZERARA et al., 2012; MCCOOL; DESISTO, 2005).

5 CONCLUSIONS

In this work, yttria-stabilized zirconia porous membranes were successfully produced by tape casting. PMMA and other additives did not affect the dispersion properties of the YSZ powder, which were governed by the adsorbed dispersant providing an electrosteric stabilization.

The pH at the isoelectric point was 7.25 for the zirconia suspension. The ceramic slurry at pH 9, yielded a zeta potential of -45 mV, confirming that the slurry was colloidally stable. The rheology behavior of the slurry was pseudoplastic, which is desirable for a tape casting process. The specific surface area value was in accordance with the results published in the literature and by the supplier.

The open porosity was controlled by using PMMA as a sacrificial pore former and by the sintering temperature. Membranes with open porosity from 27% to 51% and pore sizes in the range of 0.2 to 1.5 μm were obtained. These divergences in open porosity percentage and average pore size played a role on permeate transient flux values.

Water and n-heptane vapor adsorption showed that the membranes present a characteristic hydrophilic behavior, similar to that of oxide ceramic membranes.

Functionalization step was performed successfully and confirmed by SEM-EDX elementary analysis. The functionalized membranes showed an increase of water flux up to 5-fold.

The average pore size and porosity play a significant role in water permeability, for both functionalized and non-functionalized samples. However, the average pore size seems to have a rather stronger influence than porosity. The range of pores of the tailored surface indicated a potential application of these membranes for microfiltration processes.

6 OUTLOOK

- Permeability tests with oil/water and water/oil emulsions
- Measure the surface characteristic of the membranes after functionalization
- Explore different pore former loadings to increase the range of pore size
- Use different functional groups to generate hydrophobic surfaces

REFERENCES

ALBANO, M. P.; GARRIDO, L. B. Aqueous tape casting of yttria stabilized zirconia. **Materials Science and Engineering A**, v. 420, n. 1–2, p. 171–178, 2006.

ALBANO, M. P.; GARRIDO, L. B.; PLUCKNETT, K.; GENOVA, L. A. Processing of porous yttria-stabilized zirconia tapes: Influence of starch content and sintering temperature. **Ceramics International**, v. 35, n. 5, p. 1783–1791, 2009.

ALBANO, M. P.; GENOVA, L. A.; GARRIDO, L. B.; PLUCKNETT, K. Processing of porous yttria-stabilized zirconia by tape-casting. **Ceramics International**, v. 34, n. 8, p. 1983–1988, 2008.

ANWANDER, R.; NAGL, I.; WIDENMEYER, M.; GROEGER, O.; PALM, C.; RO, T. Surface Characterization and Functionalization of MCM-41 Silicas via Silazane Silylation. **The Journal of Physical Chemistry**, v. 104, n. 15, p. 3532–3544, 2000.

ARORA, P.; JAIN, R.; MATHUR, K.; SHARMA, A.; GUPTA, A. Synthesis of polymethyl methacrylate (PMMA) by batch emulsion polymerization. **African Journal of Pure and Applied Chemistry**, v. 4, n. 8, p. 152–157, 2010.

ASHARAF, S.; SUMA, A.; DEIVANAI, M.; MANI, R. Zirconia : properties and application — a review. **Pakistan Oral and Dental Journal**, v. 34, n. 1, p. 178–183, 2014.

BAQUERO, T.; ESCOBAR, J.; FRADE, J.; HOTZA, D. Aqueous tape casting of micro and nano YSZ for SOFC electrolytes. **Ceramics International**, v. 39, n. 7, p. 8279–8285, 2013.

BARTELS, J.; SOUZA, M. N.; SCHAPER, A.; ÁRKI, P.; KROLL, S.; REZWAN, K. Amino-Functionalized Ceramic Capillary Membranes for Controlled Virus Retention. **Environmental Science and Technology**, v. 50, n. 4, p. 1973–1981, 2016.

BELON, R.; BOULESTEIX, R.; GE, P.; MAÎTRE, A.; SALLÉ, C.; CHARTIER, T. Tape casting of multilayer YAG-Nd : YAG transparent ceramics for laser applications : Study of green tapes properties. **Journal of the European Ceramic Society**, vol. 39, n.6, p. 2161-2167, 2019.

BEROT, S.; GIRAUDET, S.; RIAUBLANC, A.; ANTON, M.; POPINEAU, Y. Key factors in membrane emulsification. **Chemical Engineering Research and Design** v. 81, n. 9, p. 1077-1082, 2003.

BOARO, M.; VOHS, J. M.; GORTE, R. J.; BOARO, M. Synthesis of Highly Porous Yttria-Stabilized Zirconia by Tape-Casting Methods. **Journal of American Ceramic Society**, v. 86, n. 3, p. 395–400, 2003.

BOTHA, P. J.; CHIANG, J. C. H.; COMINS, J. D.; MJWARA, P. M.; NGOEPE, P. E. Behavior of elastic constants , refractive index , and lattice parameter of cubic zirconia at high temperatures. **Journal of**

Applied Physics, v. 73, n. 11, p. 7268-7274, 1993.

BOUZERARA, F.; HARABI, A.; GHOUIL, B.; MEDJEMEM, N.; BOUDAIRA, B.; CONDOM, S. Elaboration and properties of zirconia microfiltration membranes. **Procedia Engineering**, v. 33, n. 2011, p. 278–284, 2012.

CALLISTER JR., W. D. **Ciencia e Engenharia dos materiais**. John Wiley & Sons, 2002.

CAUDA, V.; SCHLOSSBAUER, A.; BEIN, T. Bio-degradation study of colloidal mesoporous silica nanoparticles: Effect of surface functionalization with organo-silanes and poly(ethylene glycol). **Microporous and Mesoporous Materials**, v. 132, n. 1–2, p. 60–71, 2010.

CHEVALIER, J. What future for zirconia as a biomaterial? **Biomaterials**, v. 27, n. 4, p. 535–543, 2006.

CHEVALIER, J.; GREMILLARD, L.; VIRKAR, A. V.; CLARKE, D. R. The tetragonal-monoclinic transformation in zirconia: Lessons learned and future trends. **Journal of the American Ceramic Society**, v. 92, n. 9, p. 1901–1920, 2009.

CHHABRA, R. P. Non-Newtonian fluids: An introduction. In: **Rheology of Complex Fluids**, p. 3–34, 2010.

CHOUGUI, A.; ZAITER, K.; BELOUATEK, A.; ASLI, B. Heavy metals and color retention by a synthesized inorganic membrane. **Arabian Journal of Chemistry**, v. 7, n. 5, p. 817–822, 2014.

COSSIO, M. L. T. et al. An alternative solvent system for the steady state electrospinning of polycaprolactone. **European Polymer Journal**, v. 47, n. 6, p. 81–87, 2012.

DONG, Q.; ZHU, T.; XIE, Z.; HAN, Y.; AN, D. Optimization of the tape casting slurries for high-quality zirconia substrates. **Ceramics International**, v. 43, n. 18, p. 16943–16949, 2017.

EDER, D.; EDER, D.; KRAMER, R. Impedance spectroscopy of reduced monoclic zirconia Impedance spectroscopy of reduced monoclinic zirconia. **Physial Chemistry Chemical Physics** v. 8, n. 38, p. 4476-4483, 2014.

FLETCHER ANDREW. **Zirconia**, v. 1, 1993.

G. N. HOWATT,T R. G. BRECKENRIDGAEN, D. J. M. B. Fabrication of Thin Ceramic Sheets for Capacitors . **Journal of American Ceramic Society**, v. 30, n. 8, p. 237-242, 1947.

GESELLSCHAFT., D. K.; EMAILFACHLEUTE., V. D. **Berichte der Deutschen Keramischen Gesellschaft.**Bad Honnef. Verlag der Deutschen Keramischen Gesellschaft, 1920.

GOULART, C.; SOUZA, D. Critical analysis of aqueous tape casting , sintering, and characterization of planar Yttria-Stabilized Zirconia

electrolytes for SOFC. n. October, 2017.

HADDADA, M. BEN; BLANCHARD, J.; CASALE, S.; KRAFFT, J.; VALLÉE, A. Optimizing the immobilization of gold nanoparticles on functionalized silicon surfaces : amine- vs thiol-terminated silane **GOLD Bulletin**, v. 46, n. 4, p. 335–341, 2013.

HASSAN, M.; ABDALLAH, H. An Overview of Production and Development of Ceramic Membranes. **International Journal of Applied Engineering Research**, v. 12, n. 11, p. 7708-7721, 2016.

HEUER, A. H. Transformation Toughening in ZrO2-Containing Ceramics. **Journal of the American Ceramic Society**, v. 70, n. 10, p. 689–698, 1987.

HOOG, M. M.; RÖPKE, L.; BARTELS, J.; SOLTMANN, C.; KUNZMANN, A.; REZWAN, K.; KROLL, S. Porous ceramics with tailored pore size and morphology as substrates for coral larval settlement. **Ceramics International**, v. 44, n. 14, p. 16561–16571, 2018.

HOTZA, D. Artigo revisão: colagem de folhas cerâmicas. **Cerâmica**, v. 43, n. 283–284, p. 159–166, 1997.

HOTZA, D.; GREIL, P. Aqueous Tape Casting of Ceramic Powders. **Materials Science and Engineering: A**, v. 202, n. 1–2, p. 206–217, 1995.

HOWARTER, J. A.; YOUNGBLOOD, J. P. Optimization of silica silanization by 3-aminopropyltriethoxysilane. **Langmuir**, v. 22, n. 26, p. 11142–11147, 2006.

HOWLETT, C. R.; ZREIQAT, H.; O'DELL, R.; NOORMAN, J.; EVANS, P.; SDALTON, B. A.; MCFARLAND, C.; STEELE, J. G. The effect of magnesium ion implantation into alumina upon the adhesion of human bone derived cells. **Journal of Materials Science: Materials in Medicine**, v. 5, p. 715–722, 1994.

JABBARI, M.; BULATOVA, R.; TOK, A. I. Y.; BAHL, C. R. H.; MITSOULIS, E.; HATTEL, J. H. Ceramic tape casting: A review of current methods and trends with emphasis on rheological behaviour and flow analysis. **Materials Science and Engineering B: Solid-State Materials for Advanced Technology**, v. 212, p. 39–61, 2016.

JAVAID, A.; GONZALEZ, S. O.; SIMANEK, E. E.; FORD, D. M. Nanocomposite membranes of chemisorbed and physisorbed molecules on porous alumina for environmentally important separations. **Journal of Membrane Science**, v. 275, p. 255–260, 2006.

KELLER, J.; STAUDT, R. **Gas adsorption equilibria - Experimental methods and adsorption isotherms**. 2005.

KHARISOV, B. I.; KHARISSOVA, O. V.; DIAS, H. V. R. **Nanomaterials for Environmental Protection**. 2014.

KINGERY, W. D. Introduction to Ceramics. **Journal of The Electrochemical Society**, v. 124, n. 3, p. 152C, 1977.

KOHLER, N.; FRYXELL, G. E.; ZHANG, M. A bifunctional poly(ethylene glycol) silane immobilized on metallic oxide-based nanoparticles for conjugation with cell targeting agents. **Journal of the American Chemical Society**, v. 126, n. 23, p. 7206–7211, 2004.

KOZLOVA, D.; CHERNOUSOVA, S.; KNUSCHKE, T.; BUER, J.; WESTENDORF, A. M.; EPPLE, M. Cell targeting by antibody-functionalized calcium phosphatenanoparticles. **J. Mater. Chem.**, v. 22, n. 2, p. 396–404, 2012.

KROLL, S.; BRANDES, C.; WEHLING, J.; TRECCANI, L.; GRATHWOHL, G.; REZWAN, K. Highly efficient enzyme-functionalized porous zirconia microtubes for bacteria filtration. **Environmental Science and Technology**, v. 46, n. 16, p. 8739–8747, 2012.

KROLL, S.; TRECCANI, L.; REZWAN, K.; GRATHWOHL, G. Development and characterisation of functionalised ceramic microtubes for bacteria filtration. **Journal of Membrane Science**, v. 365, n. 1–2, p. 447–455, 2010.

LI, D.; TEOH, W. Y.; GOODING, J. J.; SELOMULYA, C.; AMAL, R. Functionalization strategies for protease immobilization on magnetic nanoparticles. **Advanced Functional Materials**, v. 20, n. 11, p. 1767–1777, 2010.

LIU, P. S.; CHEN, G. F. Chapter Two - Making Porous Metals. In: LIU, P. S.; CHEN, G. F. (Eds.). **Porous Materials**. Boston: Butterworth-Heinemann, 2014. p. 21–112.

MAHESH KUMAR, S.; ROY, S. Filtration characteristics in dead-end microfiltration of living Saccharomyces cerevisiae cells by alumina membranes. **Desalination**, v. 229, n. 1–3, p. 348–361, 2008.

MALWAL, D.; GOPINATH, P. Fabrication and applications of ceramic nanofibers in water remediation: A review. **Critical Reviews in Environmental Science and Technology**, v. 46, n. 5, p. 500–534, 2016.

MARIE, J.; BOURRET, J.; GEFFROY, P.; SMITH, A.; CHALEIX, V. Journal of the European Ceramic Society Eco-friendly alumina suspensions for tape-casting process. **Journal of the European Ceramic Society**, v. 37, n. 16, p. 5239–5248, 2017.

MATOS, M.; SUÁREZ, M. A.; GUTIÉRREZ, G.; COCA, J.; PAZOS, C. Emulsification with microfiltration ceramic membranes : A different approach to droplet formation mechanism. **Journal of Membrane** Science, v. 444, p. 345–358, 2013.

MCCOOL, B. B. A.; DESISTO, W. J. Amino-Functionalized Silica Membranes for Enhanced Carbon Dioxide Permeation. **Advanced Functional Materials,** v. 15, n. 1, p. 1635–1640, 2005.

MEDER, F.; DABERKOW, T.; TRECCANI, L.; WILHELM, M.;

SCHOWALTER, M.; ROSENAUER, A.; MÄDLER, L.; REZWAN, K. Protein adsorption on colloidal alumina particles functionalized with amino, carboxyl, sulfonate and phosphate groups. **Acta Materialia**, v. 8, n. 3, p. 1221–1229, 2012.

MIAO, X.; HU, Y.; LIU, J.; HUANG, X. Hydroxyapatite coating on porous zirconia. **Materials Science and Engineering: C**, v. 27, n. 2, p. 257–261, 2007.

MINEIRO, S. L. Processamento E Caracterização Física E Mecânica De Cerâmicas De Zircônia-Ítria Total E Parcialmente Nanoestruturadas. **Tese de Doutorado**, p. 198, 2008.

MISTLER, R. E.; TWINAME, E. R. **Tape Casting: Theory and Practice**. 2000.

MORENO, V.; AGUILAR, J. L.; HOTZA, D. 8YSZ Tapes Produced by Aqueous Tape Casting. **Materials Science Forum**, v. 727–728, n. September 2015, p. 752–757, 2012.

MORENO, V.; BERNARDINO, R. M.; HOTZA, D. Mechanical Behavior of Yttria-Stabilized Zirconia Aqueous Cast Tapes and Laminates. **Journal of Ceramics**, v. 2014, n. March, p. 1–5, 2014.

NAMGUNG, R.; ZHANG, Y.; FANG, Q. L.; SINGHA, K.; LEE, H. J.; KWON, I. K.; JEONG, Y. Y.; PARK, I. K.; SON, S. J.; KIM, W. J. Multifunctional silica nanotubes for dual-modality gene delivery and MR imaging. **Biomaterials**, v. 32, n. 11, p. 3042–3052, 2011.

NAYAK, S.; SINGH, B. P.; BESRA, L.; CHONGDAR, T. K.; GOKHALE, N. M.; BHATTACHARJEE, S. Aqueous tape casting using organic binder: A case study with YSZ. **Journal of the American Ceramic Society**, v. 94, n. 11, p. 3742–3747, 2011.

NEOUZE, M.-A.; SCHUBERT, U. Surface Modification and Functionalization of Metal and Metal Oxide Nanoparticles by Organic Ligands. **Monatshefte für Chemie - Chemical Monthly**, v. 139, n. 3, p. 183–195, 2008.

NISHIHORA, R. K.; QUADRI, M. G. N.; HOTZA, D.; REZWAN, K.; WILHELM, M. Tape casting of polysiloxane-derived ceramic with controlled porosity and surface properties. **Journal of the European Ceramic Society**, v. 38, n. 15, p. 4899–4905, 2018a.

NISHIHORA, R. K.; RACHADEL, P. L.; QUADRI, M. G. N.; HOTZA, D. Manufacturing porous ceramic materials by tape casting—A review. **Journal of the European Ceramic Society**, v. 38, n. 4, p. 988–1001, 2018b.

OLIVEIRA, A. P.; TOREM, M. L. The influence of precipitation variables on zirconia powder synthesis. **Powder Technology**, v. 119, n. 2–3, p. 181–193, 2001.

ÖZKAN, N.; OYSU, C.; BRISCOE, B. J.; AYDIN, I. Rheological analysis of ceramic pastes. **Journal of the European Ceramic Society**, v. 19, n.

16, p. 2883–2891, 1999.

PLATES, C. **Method of Producing High dielectric High Insulating ceramic plates.** n. 2582993, 1952.

PUJALA, R. K. **Dispersion Stability , Microstructure and Phase Transition of Anisotropic Nanodiscs**. 2014.

REED, J. S. **Principles of Ceramics Processing**. 2. ed. John Wiley & Sons, Inc., 1995.

RICHERSON, D. W. **The Magic of Ceramics**. 2012.

RODRIGO, A.; PARDO, F. *Processamento Viscoplástico E Conformação Cerâmica Por Rolos a Frio a Partir De Suspensões Concentradas De Alumina*. (2005). Tese (Doutorado em Ciência e Engenharia de Materiais) - Programa de Pós-graduação em Ciência e Engenharia de materiais, Universidade de São Carlos - São Paulo.

RUDAKOVA, A. V.; MAEVSKAYA, M. V.; EMELINE, A. V.; BAHNEMANN, D. W. Light-Controlled ZrO 2 Surface Hydrophilicity. **Scientific Reports**, v. 6, n. October, p. 2–6, 2016.

SANSON, A.; PINASCO, P.; RONCARI, E. Influence of pore formers on slurry composition and microstructure of tape cast supporting anodes for SOFCs. **Journal of the European Ceramic Society**, v. 28, n. 6, p. 1221–1226, 2008.

SANTA CRUZ, H.; SPINO, J.; GRATHWOHL, G. Nanocrystalline ZrO2ceramics with idealized macropores. **Journal of the European Ceramic Society**, v. 28, n. 9, p. 1783–1791, 2008.

SARIKAYA, A.; DOGAN, F. Effect of various pore formers on the microstructural development of tape-cast porous ceramics. **Ceramics International**, v. 39, n. 1, p. 403–413, 2013.

SCHICKLE, K.; KAUFMANN, R.; FILIPA, D.; CAMPOS, D.; WEBER, M.; FISCHER, H. Towards osseointegration of bioinert ceramics : Introducing functional groups to alumina surface by tailored self assembled monolayer technique. **Journal of the European Ceramic Society**, v. 32, n. 12, p. 3063–3071, 2012.

SCHNEIDER, C. A.; RASBAND, W. S.; ELICEIRI, K. W. NIH Image to ImageJ: 25 years of image analysis. **Nature Methods**, v. 9, p. 671, 28 jun. 2012.

SENTHIL KUMAR, A.; RAJA DURAI, A.; SORNAKUMAR, T. Yttria ceramics: Cutting tool application. **Materials Letters**, v. 58, n. 11, p. 1808–1810, 2004.

STUDART, A. R.; AMSTAD, E.; ANTONI, M.; GAUCKLER, L. J. Rheology of concentrated suspensions containing weakly attractive alumina nanoparticles. **Journal of the American Ceramic Society**, v. 89, n. 8, p. 2418–2425, 2006a.

STUDART, A. R.; AMSTAD, E.; GAUCKLER, L. J. Colloidal stabilization

of nanoparticles in concentrated suspensions. **Langmuir**, v. 23, n. 3, p. 1081–1090, 2007.

STUDART, A. R.; GONZENBACH, U. T.; TERVOORT, E.; GAUCKLER, L. J. Processing routes to macroporous ceramics: A review. **Journal of the American Ceramic Society**, v. 89, n. 6, p. 1771–1789, 2006b.

TAJIRI, H. A. *Manufacturing and characterization of porous ceramic capillary membranes for enzyme functionalization through click chemistry*. (2018). Dissertação (Mestrado em Engenharia Química) - Programa de Pós-graduação em Engenharia Química, Universidade Federal de Santa Catarina, Florianópolis.

TARÌ, G.; OLHERO, S. M.; FERREIRA, J. M. F. Influence of temperature on stability of electrostatically stabilized alumina suspensions. **Journal of Colloid and Interface Science**, v. 231, n. 2, p. 221–227, 2000.

TERPSTRA, R. A. **Ceramics Processing**. 1995.

TRECCANI, L.; YVONNE KLEIN, T.; MEDER, F.; PARDUN, K.; REZWAN, K. Functionalized ceramics for biomedical, biotechnological and environmental applications. **Acta Materialia**, v. 9, n. 7, p. 7115–7150, 2013.

WERNER, J.; BESSER, B.; BRANDES, C.; KROLL, S.; REZWAN, K. Production of ceramic membranes with different pore sizes for virus retention. **Journal of Water Process Engineering**, v. 4, n. C, p. 201–211, 2014.

WITZ, G.; SHKLOVER, V.; STEURER, W.; BACHEGOWDA, S.; BOSSMANN, H.-P. Phase evolution in yttria-stabilized zirconia thermal barrier coatings studied by rietveld refinement of X-ray powder diffraction patterns. **Journal of the American Ceramic Society**, v. 90, n. 7820, p. 2935–2940, 2007.

YI, J.; WANG, B.; LI, K. High performance stainless steel-ceramic composite hollow fibres for micro filtration. **Journal of Membrane Science,** v. 541, n. 5, p. 425–433, 2017.

ZHAO, X.; LIU, X.; DING, C. Acid-induced bioactive titania surface. **Journal of Biomedical Materials Research - Part A**, v. 75, n. 4, p. 888–894, 2005.

ZHOU, S.; GARNWEITNER, G.; NIEDERBERGER, M.; ANTONIETTI, M. Dispersion Behavior of Zirconia Nanocrystals and Their Surface Functionalization with Vinyl Group-Containing Ligands. n. 13, p. 9178–9187, 2007.

ZHU, Y.; WANG, D.; JIANG, L.; JIN, J. Recent progress in developing advanced membranes for emulsified oil/water separation. **NPG Asia Materials**, v. 6, n. 5, p. 101-111, 2014.

APPENDIX A – Specific BET surface areas of sintered (1300/1400/1500 °C) membranes. Isotherms obtained for two slurry compositions sintered at 1300 °C, 1400 °C and 1500 °C.